J|A|C|S
ARTICLES
Published on Web 02/10/2006

# Identification and Specificity Profiling of Protein Prenyltransferase Inhibitors Using New Fluorescent Phosphoisoprenoids

Beatrice Dursina,[†] Reinhard Reents,[†,§] Christine Delon,[†] Yaowen Wu,[†] Mahesh Kulharia,[†] Michael Thutewohl,[†,||] Alexei Veligodsky,[†,#] Alexandr Kalinin,[†,⊥] Vladimir Evstifeev,[†] Doina Ciobanu,[†] Stefan E. Szedlacsek,[‡] Herbert Waldmann,[†] Roger S. Goody,[†] and Kirill Alexandrov*[,†]

*Contribution from the Max-Planck-Institute for Molecular Physiology, Otto-Hahn-Strasse 11, 44227 Dortmund, Germany, and Department of Enzymology, Institute of Biochemistry, Spl. Independentei 296, Bucharest, 77700, Romania*

Received April 6, 2005; E-mail: kirill.alexandrov@mpi-dortmund.mpg.de

***Abstract:*** Posttranslational modification of proteins with farnesyl and geranylgeranyl isoprenoids is a widespread phenomenon in eukaryotic organisms. Isoprenylation is conferred by three protein prenyltransferases: farnesyl transferase (FTase), geranylgeranyl transferase type-I (GGTase-I), and Rab geranylgeranyltransferase (RabGGTase). Inhibitors of these enzymes have emerged as promising therapeutic compounds for treatment of cancer, viral and parasite originated diseases, as well as osteoporosis. However, no generic nonradioactive protein prenyltransferase assay has been reported to date, complicating identification of enzyme-specific inhibitors. We have addressed this issue by developing two fluorescent analogues of farnesyl and geranylgeranyl pyrophosphates {3,7-dimethyl-8-(7-nitro-benzo[1,2,5]oxadiazol-4-ylamino)-octa-2,6-diene-1}pyrophosphate (NBD-GPP) and {3,7,11-trimethyl-12-(7-nitro-benzo[1,2,5]-oxadiazo-4-ylamino)-dodeca-2,6,10-trien-1} pyrophosphate (NBD-FPP), respectively. We demonstrate that these compounds can serve as efficient lipid donors for prenyltransferases. Using these fluorescent lipids, we have developed two simple (SDS-PAGE and bead-based) in vitro prenylation assays applicable to all prenyltransferases. Using the SDS-PAGE assay, we found that, in contrast to previous reports, the tyrosine phosphatase PRL-3 may possibly be a dual substrate for both FTase and GGTase-I. The on-bead prenylation assay was used to identify prenyltransferase inhibitors that displayed nanomolar affinity for RabGGTase and FTase. Detailed analysis of the two inhibitors revealed a complex inhibition mechanism in which their association with the peptide binding site of the enzyme reduces the enzyme's affinity for lipid and peptide substrates without competing directly with their binding. Finally, we demonstrate that the developed fluorescent isoprenoids can directly and efficiently penetrate into mammalian cells and be incorporated in vivo into small GTPases.

## Introduction

The importance of covalent posttranslational modification of proteins with isoprenoids is underscored by the nature of the proteins it affects, many of which participate in signal transduction pathways controlling cell growth and differentiation, cytoskeletal rearrangement, and vesicular transport.[1] In protein prenylation, either a farnesyl or a geranylgeranyl moiety is donated by soluble phosphoisoprenoids and attached to one or two C-terminal cysteine residues of the target protein via a thioether linkage. This type of reaction can be catalyzed by three different protein prenyl transferases: protein farnesyltransferase (FTase), protein geranylgeranyl transferase-I (GGTase-I), and Rab (ras-like protein from rat brain) geranylgeranyl transferase (RabGGTase or GGTase-II) (for a review, see ref 2). The closely related FTase and GGTase-I transfer prenyl groups from prenyl pyrophosphates to proteins that contain a C-terminal CAAX motif, also known as a CAAX box (C is cysteine, A is usually an aliphatic amino acid, and X can be a variety of amino acids). The X residue of this motif largely determines the choice of the isoprenoid.

RabGGTase stands quite apart from the above-mentioned enzymes, both functionally and structurally. Like other prenyltransferases, mammalian RabGGTase is a heterodimer composed of $\alpha$- and $\beta$-subunits, the latter bearing the active site. The enzyme transfers the geranylgeranyl moiety onto two C-terminal cysteines of Rab proteins in a broad context of amino acids.[2]

[†] Max-Planck-Institute for Molecular Physiology.
[‡] Institute of Biochemistry.
[§] Present address: Pharmaceuticals Division, F. Hoffmann-La Roche Ltd., Grenzacherstrasse 124, 4070 Basel, Switzerland.
[||] Present address: Department of Chemistry, Oregon State University, 153 Gilbert Hall, Corvallis, OR 97331-4003.
[⊥] Present address: Laboratory of Skin Biology, NIAMS, NIH, 9000 Rockville Pike, Bethesda, MD 20892.
[#] Present address: Institute of Biochemistry, ETH-Zürich, Schaffmattstrasse 18, CH-8903, Zürich, Switzerland.

(1) Maurer-Stroh, S.; Washietl, S.; Eisenhaber, F. *Genome* **2003**, *4*, 212.
(2) Casey, P. J.; Seabra, M. C. *J. Biol. Chem.* **1996**, *271*, 5289−5292.


**10.1021/ja052196e CCC: $33.50** 

In contrast to other known prenyl transferases, RabGGTase does not recognize its substrate directly, but exerts its function in concert with another protein termed REP (Rab escort protein), which after prenylation escorts the Rab protein to its target membrane.[3−5]

Interest in protein prenylation was stimulated by the seminal discovery that inhibitors of farnesyltransferase can reverse transformed phenotypes of cancer cells.[6] This effect was attributed to farnesylation inhibition of the proto-oncogene Ki-Ras, which is mutated in 10−15% of human tumors. Since then, a large number of farnesyltransferase inhibitors have been tested in various stages of preclinical and clinical trials.[7,8] It was subsequently realized that the task of inhibiting Ki-Ras prenylation is more complex than was initially hoped due to the ability of GGTase-I to geranylgeranylate Ki-Ras in cells with suppressed FTase activity. This prompted development of dual inhibitors of FTase and GGTase-I.[9] Inhibitors of FTase were also tested as potential therapeutics for the treatment of sleeping sickness and other infections caused by parasitic *Trypanosomatids*.[10,11] Several lines of evidence suggest that inhibitors of GGTase-I can be effective against viral infections such as hepatitis and HIV.[12,13] A specific biphosphonate inhibitor of RabGGTase was identified and proposed as a lead compound in the development of anti-osteoporosis treatment.[14] Finally, inhibition of RabGGTase was demonstrated to be sufficient for induction of apoptosis in cancer cells.[15]

The existence of three prenyltransferases in eukaryotic cells that utilize often overlapping lipid and protein substrates may lead to cross-specificity of the inhibitors. Therefore, the ability to assess the specificity of inhibitory compounds is essential for determining their potential utility and medical applicability and calls for development of a simple assay that allows parallel assessment of numerous inhibitory activities toward all three enzymes and to a panel of protein substrates. The originally developed in vitro prenylation assay, which measures the amount of protein conjugated radioactive isoprenoid, can potentially be applied to all prenyltransferases.[16] However, it is laborious and poorly scalable. Subsequently developed farnesyltransferase assays have been based on changes in fluorescence of an N-terminally dansylated cysteine-containing pentapeptide upon farnesylation.[17] A similar assay is also used for monitoring GGTase-I activity.[18] However, several lines of evidence suggest that the latter enzyme recognizes additional epitopes upstream of the classical CAAX box and therefore use of a short peptide might produce misleading results.[19−21] The situation is more complex in the case of RabGGTase because this enzyme requires the integrity of the entire Rab protein and in particular of its switch region for its activity.[22] As a result, the activity of RabGGTase was so far assessed predominantly by radioactivity based or HPLC assays.[23,24] Although a fluorescence assay for RabGGTase was reported, it requires labor-intensive construction of fluorescent semi-synthetic protein substrates.[25]

For the reasons discussed above, the development of a generally applicable prenyltransferase assay suitable for screening large numbers of inhibitors would be desirable. Such an assay should satisfy several requirements. First, it should not be dependent on the different modes of protein substrate recognition. Second, the assay should provide an easily detectable and quantitative read-out. Third, the assay must be versatile and scalable for high-throughput applications. Fluorescence assays have been increasingly used for the identification of biologically active substances due to their high sensitivity, flexibility, and relatively low cost. However, no universally applicable fluorescence assay has been developed or proposed for the prenyltransferases despite the fact that several fluorescent analogues of both geranylgeranyl pyrophosphate (GGPP) and farnesyl pyrophosphate (FPP) have been reported.[26−28] Toward this goal, we prepared two fluorescent analogues of FPP and GGPP that were demonstrated to be efficient substrates for all three prenyltransferases. These fluorescent substrates were then used to develop a versatile on-bead microscopic assay for screening libraries of potential prenyltransferase inhibitors.

## Materials and Methods

$^1$H, $^{13}$C, and $^{31}$P spectra were recorded on a Bruker AC-250 or a Varian Mercury 400 spectrometer. The signal of the residual protonated solvent ($CDCl_3$, $CD_3OD$, or $D_2O$) was taken as reference ($^1$H, $\delta$ = 7.24 ($CHCl_3$); $^{13}$C, $\delta$ = 77.0 ($CHCl_3$)). EI and FAB mass spectra were measured on a Finnigan MAT MS 70 workstation (FAB: 3-nitrobenzyl alcohol (NBA) as matrix).

**Materials.** Flash chromatography was performed on Baker silica gel (40−65 $\mu$m) or on RP18 silica gel. All solvents were distilled using standard procedures. Commercial reagents were used without further purification.


(3) Andres, D. A.; Seabra, M. C.; Brown, M. S.; Armstrong, S. A.; Smeland, T. E.; Cremers, F. P.; Goldstein, J. L. *Cell* **1993**, *73*, 1091−1099.
(4) Alexandrov, K.; Horiuchi, H.; Steele-Mortimer, O.; Seabra, M. C.; Zerial, M. *EMBO J.* **1994**, *13*, 5262−5273.
(5) Seabra, M. C.; Brown, M. S.; Slaughter, C. A.; Sudhof, T. C.; Goldstein, J. L. *Cell* **1992**, *70*, 1049−1057.
(6) James, G. L.; Goldstein, J. L.; Brown, M. S.; Rawson, T. E.; Somers, T. C.; McDowell, R. S.; Crowley, C. W.; Lucas, B. K.; Levinson, A. D.; Marsters, J. C., Jr. *Science* **1993**, *260*, 1937−1942.
(7) Singh, S. B.; Lingham, R. B. *Curr. Opin. Drug Discovery Dev.* **2002**, *5*, 225−244.
(8) Rowinsky, E. K.; Windle, J. J.; Von Hoff, D. D. *J. Clin. Oncol.* **1999**, *17*, 3631−3652.
(9) Tucker, T. J.; et al. *Bioorg. Med. Chem. Lett.* **2002**, *12*, 2027−2030.
(10) Yokoyama, K.; Trobridge, P.; Buckner, F. S.; Van Voorhis, W. C.; Stuart, K. D.; Gelb, M. H. *J. Biol. Chem.* **1998**, *273*, 26497−26505.
(11) Buckner, F. S.; Eastman, R. T.; Nepomuceno-Silva, J. L.; Speelmon, E. C.; Myler, P. J.; Van Voorhis, W. C.; Yokoyama, K. *Mol. Biochem. Parasitol.* **2002**, *122*, 181−188.
(12) Ye, J.; Wang, C.; Sumpter, R., Jr.; Brown, M. S.; Goldstein, J. L.; Gale, M., Jr. *Proc. Natl. Acad. Sci. U.S.A.* **2003**, *100*, 15865−15870.
(13) del Real, G.; Jimenez-Baranda, S.; Mira, E.; Lacalle, R. A.; Lucas, P.; Gomez-Mouton, C.; Alegret, M.; Pena, J. M.; Rodriguez-Zapata, M.; Alvarez-Mon, M.; Martinez, A.; Manes, S. *J. Exp. Med.* **2004**, *200*, 541−547.
(14) Coxon, F. P.; Helfrich, M. H.; Larijani, B.; Muzylak, M.; Dunford, J. E.; Marshall, D.; McKinnon, A. D.; Nesbitt, S. A.; Horton, M. A.; Seabra, M. C.; Ebetino, F. H.; Rogers, M. J. *J. Biol. Chem.* **2001**, *276*, 48213−48222.
(15) Lackner, M. R.; et al. *Cancer Cell* **2005**, *7*, 325−336.
(16) Schaber, M. D.; O'Hara, M. B.; Garsky, V. M.; Mosser, S. C.; Bergstrom, J. D.; Moores, S. L.; Marshall, M. S.; Friedman, P. A.; Dixon, R. A.; Gibbs, J. B. *J. Biol. Chem.* **1990**, *265*, 14701−14704.
(17) Cassidy, P. B.; Dolence, J. M.; Poulter, C. D. *Methods Enzymol.* **1995**, *250*, 30−43.
(18) Pickett, W. C.; Zhang, F. L.; Silverstrim, C.; Schow, S. R.; Wick, M. M.; Kerwar, S. S. *Anal. Biochem.* **1995**, *225*, 60−63.
(19) Kalman, V. K.; Erdman, R. A.; Maltese, W. A.; Robishaw, J. D. *J. Biol. Chem.* **1995**, *270*, 14835−14841.
(20) Zhang, F. L.; Kirschmeier, P.; Carr, D.; James, L.; Bond, R. W.; Wang, L.; Patton, R.; Windsor, W. T.; Syto, R.; Zhang, R.; Bishop, W. R. *J. Biol. Chem.* **1997**, *272*, 10232−10239.
(21) Dursina, B. E.; Reents, R.; Niculae, A.; Veligodsky, A.; Breitling, R.; Pyatkov, K.; Waldmann, H.; Goody, R. S.; Alexandrov, K. *Protein Expression Purif.* **2005**, *39*, 71−81.
(22) Wilson, A. L.; Maltese, W. A. *J. Biol. Chem.* **1993**, *268*, 14561−14564.
(23) Seabra, M. C.; James, G. L. *Methods Mol. Biol.* **1998**, *84*, 251−260.
(24) Thoma, N. H.; Niculae, A.; Goody, R. S.; Alexandrov, K. *J. Biol. Chem.* **2001**, *276*, 48631−48636.
(25) Durek, T.; Alexandrov, K.; Goody, R. S.; Hildebrand, A.; Heinemann, I.; Waldmann, H. *J. Am. Chem. Soc.* **2004**, *126*, 16368−16378.
(26) Kim, M.; Kleckley, T. S.; Wiemer, A. J.; Holstein, S. A.; Hohl, R. J.; Wiemer, D. F. *J. Org. Chem.* **2004**, *69*, 8186−8193.
(27) Owen, D. J.; Alexandrov, K.; Rostkova, E.; Scheidig, A. J.; Goody, R. S.; Waldmann, H. *Angew. Chem., Int. Ed.* **1999**, *38*, 509−512.
(28) Liu, X. H.; Prestwich, G. D. *J. Am. Chem. Soc.* **2002**, *124*, 20−21.

**2-[2,6,10-Trimethyl-12-(tetrahydropyrane-2-yloxy)-dodeca-2,6,-10-trienyl]-isoindol-1,3-dione (Pht-F-OTHP).** To a solution of phthalimide (204 mg, 1.39 mmol), triphenylphosphine (364 mg, 1.39 mmol), and 2,6,10-trimethyl-12-(tetrahydropyrane-2-yloxy)-dodeca-2,6,-10-trien-1-ol[29−31] (448 mg, 1.39 mmol) in THF (1 mL) was added diethylazodicarboxylat (DEAD) (242 mg, 1.39 mmol). The reaction was left stirring for 12 h, and the solvent was removed in vacuo. The residue was taken up in diethyl ether (50 mL), filtered, and the solvent was removed in vacuo. Purification of the resulting oil by flash chromatography using *n*-hexane/ethyl acetate (6:1) as eluent yielded 497 mg (1.10 mmol, 79%) of the desired product as a colorless oil. $R_f$ 0.30 (*n*-hexane/ethyl acetate, 3:1). $^1$H NMR (400 MHz, $CDCl_3$): $\delta$ = 1.55 (s, 3H); 1.63 (s, 3H); 1.64 (s, 3H); 1.49−1.70 (m, 6H); 1.94−2.15 (m, 4H); 3.48−3.50 (m, 1H); 3.85−3.89 (m, 1H); 3.90−4.08 (m, 1H); 4.17 (s, 2H); 4.10−4.30 (m, 1H); 4.61 (t, $J$ = 3.5 Hz, 1H); 5.03−5.08 (m, 1H); 5.32−5.34 (m, 2H); 7.70 (m, 2H); 7.83 (m, 2H). $^{13}$C NMR (100.6 MHz, $CDCl_3$): $\delta$ = 14.6 ($CH_3$); 16.0 ($CH_3$); 16.4 ($CH_3$); 19.6 ($CH_2$); 25.5, 26.2, 26.4 ($CH_2$); 30.7 ($CH_2$); 39.1 ($CH_2$); 39.5 ($CH_2$); 44.9 ($CH_2$); 62.2−63.6 ($CH_2$); 97.7 (CH); 120.5 (CH); 123.2 (CH); 124.2 (CH); 127.4 (CH); 129.1 ($C_q$); 132.1 ($C_q$); 133.9 (CH); 134.7 ($C_q$); 140.2 ($C_q$); 168.2. MS (FAB, 3-NBA): *m*/*z* calcd for $[M + Na]^+$, 474.2723; found, 474.2682; $C_{28}H_{37}NO_4$ (451.6).

**2,6,10-Trimethyl-12-(tetrahydropyrane-2-yloxy)-dodeca-2,6,10-trienylamine ($H_2$N-F-OTHP) (1b).** To a solution of Pht-Far-OTHP (497 mg, 1.29 mmol) in ethanol (30 mL) was added hydrazine (387 mg, 7.74 mmol). The reaction was left stirring for 12 h, filtered, and the solvent was removed in vacuo. Purification of the resulting oil by flash chromatography using ethyl acetate/triethylamine (99:1) as eluent yielded 393 mg (1.22 mmol, 95%) of the desired product **1b** as a yellowish oil. $R_f$ 0.24 (ethyl acetate/triethylamine (99:1)). $^1$H NMR (250 MHz, $CDCl_3$): $\delta$ = 1.61 (s, 3H); 1.64 (s, 3H); 1.68 (s, 3H); 1.40−1.90 (m, 6H); 2.07 (m, 8H); 3.16 (s, 2H); 3.52 (m, 1H); 3.90 (m, 1H); 4.03 (dd, $J$ = 11.8 Hz, $J$ = 7.4 Hz, 1H); 4.24 (dd, $J$ = 11.8 Hz, $J$ = 6.4 Hz, 1H); 4.63 (t, $J$ = 3.3 Hz, 1H); 5.12 (t, $J$ = 6.2, 1H); 5.26 (t, $J$ = 6.8, 1H); 5.36 (t, $J$ = 6.9, 1H). $^{13}$C NMR (100.6 MHz, $CDCl_3$): $\delta$ = 14.4 ($CH_3$); 15.9 ($CH_3$); 16.3 ($CH_3$); 19.5 ($CH_2$); 25.4, 26.1, 26.2 ($CH_2$); 30.6 ($CH_2$); 39.4 ($CH_2$); 39.5 ($CH_2$); 44.9 ($CH_2$); 62.1−63.5 ($CH_2$); 97.6 (CH); 120.5 (CH); 123.4 (CH); 123.9 (CH); 135.1 ($C_q$); 137.2 ($C_q$); 140.2 ($C_q$). MS (FAB, 3-NBA): *m*/*z* calcd for $[M + H]^+$, 322.2688; found, 322.2725; $C_{20}H_{35}NO_2$ (321.5).

**7-Nitrobenzo[1,2,5]oxadiazol-4-yl-1-[2,6,10-trimethyl-12-(tetrahydro-pyrane-2-yloxy)-dodeca-2,6,10-trienyl]-amine (NBD-NH-F-OTHP) (2b).** To a solution of $H_2$N-F-OTHP (**1b**) (393 mg, 1.22 mmol) in acetonitrile/25 mM $NaHCO_3$ buffer (1:1) (15 mL) was slowly added a solution of NBD-Cl (365 mg, 1.83 mmol) in acetonitrile (5 mL). After the mixture was stirred for 1 h, further NBD-Cl (365 mg, 1.83 mmol) was added. The mixture was left stirring for 1 h. The resulting black solution was poured into a separating funnel containing dichloromethane and brine solution. The layers were separated, dried over $Na_2SO_4$, filtered, and the solvent was removed in vacuo. Purification of the resulting oil by flash chromatography using methylene chloride as eluent yielded 384 mg (0.79 mmol, 65%) of the desired product **2b** as a reddish brown oil. $R_f$ 0.10 (methylene chloride). $^1$H NMR (250 MHz, $CDCl_3$): $\delta$ = 1.54 (s, 3H); 1.61 (s, 3H); 1.69 (s, 3H); 1.46−1.81 (6H, m); 1.96−2.20 (m, 8H); 3.47 (m, 1H); 3.86 (m, 1H); 3.98 (dd, $J$ = 11.9 Hz, $J$ = 4.8 Hz, 1H); 4.02 (d, $J$ = 6.0 Hz, 2H); 4.19 (dd, $J$ = 11.9 Hz, $J$ = 6.5 Hz, 1H); 4.58 (dd, $J$ = 2.2 Hz, $J$ = 2.2 Hz, 1H); 5.04 (tq, $J$ = 6.4 Hz, $J$ = 0.9 Hz, 1H); 5.29 (ddq, $J$ = 6.5 Hz, $J$ = 4.8 Hz, $J$ = 1.0 Hz, 1H); 5.45 (tq, $J$ = 6.5 Hz, $J$ = 1.0 Hz, 1H); 6.16 (d, $J$ = 8.7 Hz, 1H); 6.81 (t, $J$ = 6.0, 1H); 8.42 (d, $J$ = 8.7 Hz, 1H). $^{13}$C NMR (100.6 MHz, $CDCl_3$): $\delta$ = 14.5 ($CH_3$); 15.9 ($CH_3$); 16.3 ($CH_3$); 19.6 ($CH_2$); 25.4, 26.1, 26.2 ($CH_2$); 30.6 ($CH_2$); 38.9 ($CH_2$); 39.4 ($CH_2$); 51.4 ($CH_2$); 62.3−63.6 ($CH_2$); 97.8 (CH); 98.5 (CH); 120.6 (CH); 123.5 (CH); 124.4 (CH); 128.9 ($C_q$); 136.5 (CH); 128.6, 134.4, 139.9, 143.8, 144.2 ($C_q$). MS (EI): *m*/*z* calcd for $[M + H]^+$, 484.2686; found, 484.2707; $C_{26}H_{36}N_4O_5$ (484.6).

**3,7,11-Trimethyl-12-(7-nitro-benzo[1,2,5]oxadiazo-4-ylamino)-dodeca-2,6,10-trien-1-ol (NBD-NH-F-OH) (3b).** To a solution of NBD-NH-F-OTHP (**2b**) (384 mg, 0.79 mmol) in ethanol was added PPTS (460 mg, 1.63 mg). The reaction was heated at 60°C for 3 h, and poured into a separating funnel containing diethyl ether and brine solution. The layers were separated, dried over $Na_2SO_4$, filtered, and the solvent was removed in vacuo. Purification of the resulting oil by flash chromatography using *c*-hexane/ethyl acetate (1.5:1) as eluent yielded 298 mg (0.74 mmol, 94%) of the desired product **3b** as a reddish brown oil. $R_f$ 0.23 (*n*-hexane/ethyl acetate (1.5:1)). $^1$H NMR (250 MHz, $CDCl_3$): $\delta$ = 1.59 (br, 3H); 1.67 (br, 3H); 1.73 (br, 3H); 1.95−2.30 (m, 8H); 4.02 (d, $J$ = 5.5 Hz, 2H); 4.18 (d, $J$ = 6.8 Hz, 2H); 5.08 (tq, $J$ = 6.9 Hz, $J$ = 1.1 Hz, 1H); 5.38 (tq, $J$ = 7.4 Hz, $J$ = 1.2 Hz, 1H); 5.46 (tq, $J$ = 7.1 Hz, $J$ = 1.2 Hz, 1H); 6.17 (d, $J$ = 8.7 Hz, 1H); 6.84 (br, 1H); 8.46 (d, $J$ = 8.7 Hz, 1H). $^{13}$C NMR (100.6 MHz, $CDCl_3$): $\delta$ = 14.7 ($CH_3$); 15.9 ($CH_3$); 16.3 ($CH_3$); 26.0, 26.1 ($CH_3$); 38.9−39.4 ($CH_2$); 51.3 ($CH_2$); 59.5 ($CH_2$); 99.2 (CH); 123.4 (CH); 124.5 (CH); 136.5 (CH); 123.8, 128.6, 134.4, 139.3, 143.9, 144.2, 144.3 ($C_q$). MS (EI): *m*/*z* calcd for $[M + H]^+$, 400.2111; found, 400.2099; $C_{21}H_{28}N_4O_4$ (400.5).

**(12-Chloro-2,6,10-trimethyl-dodeca-2,6,10-trienyl)-(7-nitro-benzo-[1,2,5]oxadiazol-4-yl)amine 4b (NBD-NH-F-Cl).** To a solution of *N*-chlorosuccinimide (111.3 mg, 0.83 mmol) in dichloromethane (8 mL), stirring at −40 °C under an atmosphere of argon, was added dimethyl sulfide (92.4 mg, 1.49 mmol) dropwise. The reaction was then warmed to 0 °C with an ice bath and kept at this temperature for 5 min. The reaction was then cooled back to −40 °C, and a solution of NBD-NH-Far-OH (**3b**) (298 mg, 0.74 mmol) in dichloromethane (8 mL) was added dropwise. The resulting muddy black solution was then left stirring to warm to 0 °C over 1 h. The reaction was maintained at 0 °C for another hour, after which time it was then warmed to room temperature for a further 15 min. The resulting solution was poured into a separating funnel containing diethyl ether (100 mL) and ice-cold brine solution. The layers were separated, and the organic phase was washed once with ice-cold brine solution. The combined aqueous phases were back extracted with diethyl ether (2 × 20 mL). The combined organic phase was dried over $Na_2SO_4$, filtered, and the solvent was removed in vacuo, to yield 315 mg (0.74 mmol, quant.) of **4b** as a reddish brown oil. $R_f$ 0.45 (*n*-hexane/ethyl acetate (3:1)). $^1$H NMR (250 MHz, $CDCl_3$): $\delta$ = 1.55 (br, 3H); 1.67 (d, $J$ = 1.0, 3H); 1.70 (br, 3H); 1.96−2.16 (m, 8H); 4.03 (d, $J$ = 7.8 Hz, 2H); 4.05 (d, $J$ = 8.0 Hz, 2H); 5.04 (tq, $J$ = 6.4 Hz, $J$ = 1.0 Hz, 1H); 5.38 (tq, $J$ = 8.0 Hz, $J$ = 1.2 Hz, 1H); 5.47 (tq, $J$ = 6.6 Hz, $J$ = 0.9 Hz, 1H); 6.18 (d, $J$ = 8.7 Hz, 1H); 6.78 (d, $J$ = 5.8, 1H); 8.41 (d, $J$ = 8.7 Hz, 1H). $^{13}$C NMR (100.6 MHz, $CDCl_3$): $\delta$ = 14.5 ($CH_3$); 15.9 ($CH_3$); 25.9−26.2 ($CH_2$); 38.9−39.2 ($CH_2$); 41.1 ($CH_2$); 51.4 ($CH_2$); 99.3 (CH); 120.2 ($CH_2$); 123.9 (CH); 129.1 (CH); 136.6 (CH); 123.4, 128.6, 134.7, 142.5, 143.8, 144.2 ($C_q$). MS (FAB, 3-NBA): *m*/*z* calcd for $[M + H]^+$, 419.1772; found, 419.1760; $C_{21}H_{27}N_4O_3Cl$ (418.9).

**Synthesis of Tris-ammonium{3,7-dimethyl-8-(7-nitro-benzo-[1,2,5]oxadiazol-4-ylamino)-octa-2,6-diene-1}pyrophosphate (NBD-GPP) (7a).** Tris(tetra-*N*-butylammonium) pyrophosphate (**5**)[32] (1.76 g, 1.85 mmol) was dissolved in acetonitrile (8 mL) under an argon atmosphere. NBD-NH-Ger-Cl (**4a**)[33] (100 mg, 284 $\mu$mol) was added to the resulting solution, and the reaction mixture was stirred at ambient temperature for 2.5 h.[32] The mixture was then concentrated by rotary evaporation, and the residue was dissolved in 5 mL of 25 mM

(29) Turek, T. C.; Gaon, I.; Gamache, D.; Distefano, M. D. *Bioorg. Med. Chem. Lett.* **1997**, *7*, 2125−2130.
(30) Vig, O. P.; Sharma, M. L.; Gauba, R.; Puri, S. K. *Indian J. Chem.* **1985**, *24*, 513−515.
(31) Umbreit, M. A.; Sharpless, K. B. *J. Am. Chem. Soc.* **1977**, *99*, 5526−5528.
(32) Davidsson, V. J.; Woodside, A. B.; Neal, T. R.; Stremler, K. E.; Muehlbacher, M.; Poulter, C. D. *J. Org. Chem.* **1986**, *51*, 4768−4779.
(33) Reents, R.; Wagner, M.; Schlummer, S.; Kuhlmann, J.; Waldmann, H. *ChemBioChem* **2005**, *6*, 86−94.

ammonium bicarbonate buffer/2-propanol 19:1 [v:v]. The resulting solution was rapidly passed through a 2 × 8 cm Dowex AG50x8 ion exchange column ($NH_4^+$ form). Lyophilization of the eluent yielded an orange solid, which was dissolved in 2 mL of 25 mM ammonium bicarbonate. This resulting mixture was purified by flash chromatography on an RP 18 silica gel with a linear gradient elution starting from 25 mM ammonium bicarbonate buffer to acetonitrile. The fractions containing **7a** were collected, and acetonitrile was removed by rotary evaporation. Lyophilization of the resulting material afforded 106 mg (196 $\mu$mol, 69%) of pure **7a** as a fluffy, hygroscopic orange solid. $^1$H NMR (250 MHz, $D_2O$): $\delta$ = 1.52 (s, 6H); 1.94 (t, $J$ = 7.3 Hz, 2H); 2.04 (td, $J$ = 7.3 Hz, $J$ = 7.0 Hz, 2H); 3.90 (s, 2H); 4.29 (t, $J$ = 6.9 Hz, 2H); 5.26 (t, $J$ = 6.9 Hz, 1H); 5.32 (t, $J$ = 7.0 Hz, 1H); 6.13 (d, $J$ = 8.7 Hz, 1H); 8.25 (d, $J$ = 8.7 Hz, 1H). $^{31}$P NMR (200 MHz, $D_2O$): $\delta$ = −9.50 (d, 1P), −7.90 (d, 1P). MS (FAB, 3-NBA): *m/z* calculated for $[M - H]^-$, 491.0811; found, 491.0698; $C_{16}H_{31}N_7O_{10}P_2$ (543.4).

**Synthesis of Tris-ammonium{3,7,11-trimethyl-12-(7-nitro-benzo-[1,2,5]oxadiazo-4-ylamino)-dodeca-2,6,10-trien-1}pyrophosphate (NBD-FPP) (7b).** Compound **7b** was prepared using NBD-NH-Far-Cl (**4b**) (79.0 mg, 186 $\mu$mol) and tris(tetra-*N*-butylammonium) pyrophosphate[32] (1.17 g, 1.23 mmol) as described for the synthesis of **7a**. Compound **7b** was obtained as a fluffy, hygroscopic orange solid (62.0 mg (115 $\mu$mol, 61%)). $^1$H NMR (250 MHz, $D_2O$): $\delta$ = 1.26 (br, 3H); 1.41 (br, 3H); 1.46 (br, 3H); 1.68−1.87 (m, 8H); 3.87 (m, 2H); 4.25 (t, $J$ = 6.8 Hz, 2H); 5.10 (t, $J$ = 6.9 Hz, 1H); 5.13−5.25 (m, 2H); 6.07 (d, $J$ = 8.7 Hz); 8.19 (d, $J$ = 8.7 Hz, 1H). $^{31}$P NMR (200 MHz, $D_2O$): $\delta$ = −9.20 (m, 1P), −5.40 (m, 1P). MS (FAB, 3-NBA): *m/z* calcd for $[M(C_{21}H_{30}N_4O_{10}P_2) + NH_4^+]^-$, 578.1781; found, 578.1921; $C_{21}H_{39}N_7O_{10}P_2$ (611.5).

**Synthesis of the Compound Library.** Investigated members of the tripeptide library 343, 621, 623, 656, 651, 650, 669, 670, 672, and 673 were synthesized in a parallel approach and isolated as pure compounds as described before.[34] The FTase inhibitor B581 was purchased from EMD Biosciences.[35]

**Construction of Expression Vectors for Small GTPases.** Open reading frames of canine Rab7, human Rab1A, RhoA, and Ki-Ras were amplified by PCR with specific primers carrying *Nde*I and *Xho*I restriction sites. PCR products were digested with *Nde*I and *Xho*I and inserted into the pGATEV vector predigested with the same enzymes.[36] The integrity of the open reading frames was verified by nucleotide sequencing.

**Construction of Expression Vectors for Prenyltransferases.** The two-vector expression system for RabGGTase was described earlier.[36] For construction of expression systems for GGTase-I and FTase, an identical strategy was employed. The cDNA for the α subunit of FTase was inserted between the *Nde*I and *Xho*I sites of the pGATEV vector, and the $\beta$ subunits of GGTase-I and FTase were cloned between the *Nde*I and *Xho*I sites of pET30 expression vector.

**Expression and Purification of Glutathione-*S*-transferase (GST)-GTPase Fusion Proteins.** Expression vectors for substrate GTPases were transformed into competent *E. coli* BL21(DE3) Codon Plus RIL cells, and high-level expression of fusion proteins was induced by the addition of IPTG to suspension cultures to a final concentration of 0.2 mM at the $OD_{600}$ 0.9, and then incubated at 20 °C for 12 h. Cells were lysed in lysis buffer (50 mM $Na_2HPO_4$ pH 8.0, 0.3 M NaCl, and 2 mM $\beta$-mercaptoethanol (BME), 1 mM phenylmethylsulfonylfluoride (PMSF)) by passing twice through a fluidizer (Microfluidics). The resulting homogenate was clarified by centrifugation (30 000*g*, 1 h at 4 °C) and filtered through a 0.45 $\mu$m nitrocellulose filter (Schleicher and Schuell). The filtrate was loaded onto a 5 mL Hi-Trap Ni Sepharose column (Pharmacia) pre-equilibrated with the lysis buffer. The column was washed extensively with lysis buffer containing 5 mM imidazol, and the bound protein was eluted with a linear 5−200 mM imidazol gradient in 30 column volumes. Fractions containing GST-GTPases were pooled. In some cases, proteins were further purified by gel filtration on a 26/60 Superdex 200 column (Pharmacia) equilibrated with buffer containing 25 mM HEPES pH 7.2, 25 mM NaCl, 5 mM DTT, 2 mM $MgCl_2$, and 200 $\mu$M guanosine diphosphate (GDP), concentrated to ca. 10 mg/mL and stored in multiple aliquots at −80 °C.

**Expression and purification of protein tyrosine phosphatase PRL-3** was performed according to a slightly modified version of the procedure reported earlier.[37] Briefly, the PRL overexpressing *E. coli* cells were resuspended in a phosphate buffered saline (PBS) buffer (pH 7.4) supplemented with 20 mM imidazol and 1 mM PMSF. The cell-free extract was applied on a Hi Trap Ni Chelating column (Amersham Biosciences), and, after extensive washing, the bound protein was eluted using a gradient of 20−500 mM imidazole. Fractions containing electrophoretically homogeneous PRL-3 were collected, and finally the buffer was changed to the storage buffer (50 mM Tris pH 7.5, 150 mM NaCl, 1 mM DTT).

**Expression and purification of prenyltransferases** was performed essentially as described for RabGGTase.[36] For the expression of FTase, the expression temperature was raised to 37 °C and the expression time was shortened to 4 h.

**SDS-PAGE-Based Prenyltransferase Assay.** 5 $\mu$M protein substrate (RhoA, Ki-Ras4B, Rab1, or Rab7 fused to GST) was incubated with 5 $\mu$M of the appropriate prenyltransferase (GGTase-I, FTase, or RabGGTase, respectively) and 25 $\mu$M NBD-GPP or NBD-FPP in the prenylation buffer (50 mM Hepes pH 7.2, 50 mM NaCl, 5 mM DTT, 5 mM $MgCl_2$, 20 $\mu$M GDP) in a final volume of 20 $\mu$L. When Rab proteins were used as protein substrate, REP-1 was also added to the mixture to a final concentration of 6 $\mu$M. Control reactions were supplemented with a 5-fold excess of GGPP or FPP over the fluorescent lipid, which prevents incorporation of fluorescent analogues into protein substrate due to higher concentration and affinity of the native isoprenoids for prenyltransferase (see Results and Discussion). The ratio of unlabeled to labeled isoprenoids required for >90% inhibition of NBD-isoprenoid incorporation was determined by titrating a standard prenylation reaction with increasing concentrations of either GGPP or FPP. The reaction mixtures were incubated for 15 min at room temperature and then quenched by addition of 20 $\mu$L of hot 2x SDS-PAGE sample buffer. The samples were boiled at 95 °C for 3 min, and 25 $\mu$L was loaded onto 15% SDS-PAGE. The fluorescent bands corresponding to the prenylated proteins were visualized in the gel using a Fluorescent Image Reader FLA-5000 (Fuji) (excitation laser, 473 nm; cutoff filter, 510 nm) followed by staining with Coomassie blue and scanning.

**Analysis of Prenylation by Fluorescent Lipids Using Steady-State Kinetics.** FTase, GGTase-I, and RabGGTase steady-state kinetics were assayed by quantitating the amount of NBD-prenylated GST-Ki-Ras, GST-RhoA, or Rab7 products respectively on SDS-PAGE as described above. A typical reaction contained various concentrations of fluorescent isoprenoids or various concentrations of protein substrate in 25 mM Hepes, pH 7.2, 40 mM NaCl, 2 mM $MgCl_2$, 2 mM DTT, 100 $\mu$M GDP. After pre-equilibration of the assay mixture at 30 °C in the absence of enzyme, the reaction was initiated by the addition of the prenyltransferase transferase to a final concentration of 2−20 nM. At time intervals, aliquots of 10 $\mu$L were withdrawn, and the reaction was stopped by the addition of Laemmli sample buffer and analyzed by

(34) Thutewohl, M.; Kissau, L.; Popkirova, B.; Karaguni, I. M.; Nowak, T.; Bate, M.; Kuhlmann, J.; Muller, O.; Waldmann, H. *Bioorg. Med. Chem.* **2003**, *11*, 2617−2626.
(35) Cox, A. D.; Garcia, A. M.; Westwick, J. K.; Kowalczyk, J. J.; Lewis, M. D.; Brenner, D. A.; Der, C. J. *J. Biol. Chem.* **1994**, *269*, 19203−19206.
(36) Kalinin, A.; Thoma, N. H.; Iakovenko, A.; Heinemann, I.; Rostkova, E.; Constantinescu, A. T.; Alexandrov, K. *Protein Expression Purif.* **2001**, *22*, 84−91.
(37) Matter, W. F.; Estridge, T.; Zhang, C.; Belagaje, R.; Stancato, L.; Dixon, J.; Johnson, B.; Bloem, L.; Pickard, T.; Donaghue, M.; Acton, S.; Jeyaseelan, R.; Kadambi, V.; Vlahos, C. J. *Biochem. Biophys. Res. Commun.* **2001**, *283*, 1061−1068.

SDS-PAGE. The fluorescence of the bands corresponding to the prenylated GTPases was scanned as described above and was quantitatively analyzed using AIDA densitometry software.

**Bead-Based Prenyltransferase Assay.** The GST-fusion GTPases (GST-Ki-Ras, GST-Rab7, or GST-RhoA) were immobilized on glutathione-Sepharose beads. For this purpose, 130 $\mu$L of glutathione-Sepharose 4B beads (Amersham Biosciences) 75% slurry in ethanol was dispensed and equilibrated with binding buffer PBS (137 mM NaCl, 2.7 mM KCl, 4.3 mM $Na_2HPO_4$, 1.4 mM $KH_2PO_4$, pH 7.3). The beads were pelleted by centrifugation at 500*g* for 5 min in a benchtop centrifuge, and the supernatant was discarded. For binding, the resulting approximately 100 $\mu$L of drained beads was incubated with 0.5 mg of GST-Ki Ras4B, GST-Rab7, or GST-RhoA in PBS in a final volume of 1 mL. After 30 min of incubation at room temperature, the beads were harvested by centrifugation at 500*g* for 5 min. The unbound GST-fusion protein was removed by washing the beads three times with 10 bed volumes of fresh PBS. Approximately 0.3 mg of GST-tagged protein was immobilized on 100 $\mu$L of drained beads. To correct for differences in binding efficiencies of proteins to the matrix and to compensate for potential loss during washing and handling steps, the amount of the GTPase substrates used in the bead assay was increased to 1:20 molar ratio with respect to prenyltransferase.

To perform the prenylation reaction, the beads were then equilibrated with reaction buffer (50 mM Hepes pH 7.2, 50 mM NaCl, 5 mM DTT, 5 mM $MgCl_2$, 20 $\mu$M GDP) and finally resuspended in 200 $\mu$L of the same buffer. This resulted in an approximately 30% slurry. For a typical bead-based prenylation reaction, 10 $\mu$L of a 30% slurry of glutathione-Sepharose bound GST-GTPase was incubated with 3 $\mu$M of the appropriate prenyltransferase, 10 $\mu$M NBD-GPP or NBD-FPP, and 200 $\mu$M synthetic inhibitor. In the case of GST-Rab7, REP-1 was also added to a final concentration of 6 $\mu$M. The total reaction volume was brought to 20 $\mu$L with prenylation buffer. In parallel, positive control reactions (no inhibitor) were carried out. The reaction mixtures were incubated for 8 min at 25 °C in a Thermo mixer (Eppendorf) with continuous agitation (800 rpm). The reactions were stopped by addition of 500 $\mu$L of cold prenylation buffer, diluting the reaction mixture 25-fold. The beads were immediately pelleted by short spinning in a benchtop centrifuge and washed three times with the same buffer. Finally, the beads were resuspended in 20 $\mu$L of buffer, spread on a glass slide, covered with cover slips, and visualized using a fluorescence microscope (Axiophot, Zeiss, Germany). The NBD fluorescence was visualized using the Zeiss filter set for FITC because this fluorophor has spectral characteristics closest to those of NBD.

The images were acquired through a 10× Plan-Neofluar objective using an AxioCam CCD camera (Carl Zeiss Vision GmbH, Germany). The exposure time was 10 s in all cases. The software used to record images was Axio Vision 2.05 (Zeiss).

**$IC_{50}$ Determination.** 3 $\mu$M GST-tagged GTPase was incubated for 4 min at room temperature with 1 $\mu$M prenyltransferase, 10 $\mu$M fluorescent lipid, and increasing concentrations of inhibitor. The reactions were stopped by addition of sample buffer and resolved on SDS-PAGE. The fluorescence of the bands corresponding to the prenylated GTPases was quantitatively analyzed using AIDA densitometry software, and the values were corrected for pipeting errors using Comassie blue staining of the same bands. The data were fitted using a quadratic equation equivalent to that given below for fluorescence titrations.

**Fluorescence Measurements.** Fluorescence spectra and long time base fluorescence measurements were performed with an Aminco SLM 8100 spectrophotometer (Aminco). All reactions were followed at 25 °C in 50 mM Hepes pH 7.2, 50 mM NaCl, and 5 mM DTT in a volume of 1 mL. The NBD fluorescence was excited at 487 nm, and data were collected at 530 nm for the interaction with GGTase-I or at 550 nm for the interaction with FTase and RabGGTase. Data analysis was performed with the program Grafit 4.0 (Erithacus Software). To estimate the affinity of the recombinant enzymes for phosphoisoprenoids, solutions of 20, 50, or 200 nM fluorescent isoprenoid diphosphate were titrated with recombinant prenyltransferase. Titrations were fitted using the quadratic equation describing the fluorescence change expected under these conditions:

$$F_{\min} + \frac{(F_{\max} - F_{\min}) \times [(P + L + K) - \sqrt{(P + L + K)^2 - 4pl}]}{2p}$$

where $F$ is the fluorescence intensity (in arbitrary units), $F_{\min}$ is the intensity at the beginning of the titration, $F_{\max}$ is the fluorescence intensity of the complex, $P$ is the total NBD-isoprenoid concentration, $L$ is the prenyltransferase concentration, and $K$ is the dissociation constant for the interaction. In the fit to this equation, $F_{\min}$, $F_{\max}$, $P$, and $K_d$ were allowed to vary in the program Grafit (Erithacus Software).[38]

For the competive titration of GGTase-I with NBD-FPP and GGPP, fits were performed with the program Scientist (Micromath) using a model file that allows simulation and fitting to the set of three equations describing the two equilibria and the generation of the fluorescence signal (for details, see ref 39). The $K_d$ value for the GGTase-I:NBD-FPP interaction was held constant at the value determined from the direct titration.

**Cell Culture.** Human epidermal carcinoma A431 cells were cultured in Dulbecco's modified Eagle's medium (Sigma) supplemented with 10% fetal bovine serum, 4 mM L-glutamine, and 4.5 g/L glucose and were adjusted to contain 1.5 g/L sodium bicarbonate. Cells were passaged every 4 days. COS-7 cells were grown in DMEM medium with glutamine (Invitrogen) with 10% fetal bovine serum, and penicillin/streptomycin. Cells were passaged every 3 days.

**Intracellular Delivery and Imaging of the NBD-Isoprenoids.** Subconfluent A431 cells grown on glass cover slips were incubated on ice or at 37 °C with 10 $\mu$M NBD-FPP or NBD-GPP added directly to the growth medium, washed three times with PBS fixed for 10 min in 4% formaldehyde diluted in PBS, and mounted onto object slides. Cell imaging was done using a Nikon Eclipse 80i confocal microscope with a green (488 nm) excitation laser.

**Transfection of COS-7 Cells with EYFP-Ki-Ras and ECFP-GDI and Detection of in Vivo Prenyltransferase Activity.** The vector pH2b_GDI_ECFP_Tev_EYFP_Ki_Ras is a derivative of pHcRed1-N1 (Clontech) designed to coexpress ECFP-GDI and EYFP-Ki-Ras fusion proteins and will be described elsewhere (Delon and Alexandrov, unpublished). For in vivo prenylation experiments, COS-7 cells were grown in 12-well dishes to 70% confluence and incubated for 2 h with 200 $\mu$g of plasmid DNA mixed with 200 $\mu$g/mL DEAE dextran per well. This was followed by a 4.5 h incubation of the cells with 100 $\mu$g of chloroquine to inhibit lysosomal degradation and allow DNA to escape from lysosomes and enter the nucleus. Approximately 24 h after transfection, cells were rinsed with fresh medium and compactin was added to the medium at 20 $\mu$M. After 24 h of incubation with compactin, fluorescent isoprenoids were added to a final concentration of 100 $\mu$M to the medium and cells were incubated for an additional 6 h. In control experiments, cells were incubated with 50 $\mu$M of GGPP or FPP in addition to fluorescent isoprenoids. Following the incubation, cells were lysed and resolved on 12% SDS-PAGE gel. The fluorescent bands were visualized using a fluorescent image reader (FLA-5000) as described above.

## Results and Discussion

**Synthesis of Fluorescent Analogues of FPP and GGPP.** The fluorescent 7-nitro-benzo[1,2,5]oxadiazol-4-ylamino (NBD) group[40] was chosen because it is one of the smallest known

(38) Thoma, N. H.; Iakovenko, A.; Owen, D.; Scheidig, A. S.; Waldmann, H.; Goody, R. S.; Alexandrov, K. *Biochemistry* **2000**, *39*, 12043−12052.
(39) Alexandrov, K.; Scheidig, A. J.; Goody, R. S. *Methods Enzymol.* **2001**, *329*, 14−31.
(40) Ghosh, P. B.; Whitehou, M. W. *Bochem. J.* **1968**, *108*, 155.

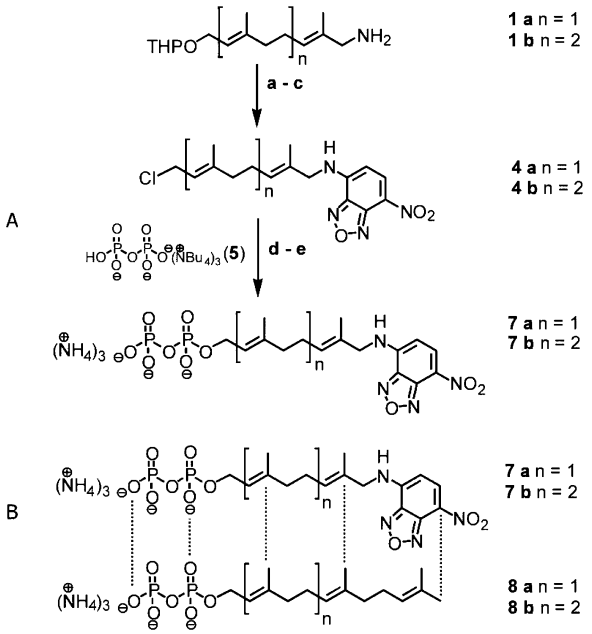


***Figure 1.*** (A) Synthesis of fluorescent diphosphates **7a** and **7b**: (a) NBD-Cl, $NaHCO_3$ buffer (pH 8−9), $CH_3CN$; 67−65%; (b) PPTS, 60 °C, EtOH; 93−94%; (c) NCS, DMS, −30 → 0 °C, **4a** = quant.; **4b** = quant.; (d) **5**, $CH_3CN$, room temperature, 3 h; (e) DOWEX ion exchange $NBu_4^+/NH_4^+$; **7a** = 69%; **7b** = 61%. (B) Comparison of the fluorescent isoprenoid analogues with the native phosphoisoprenoids.

compounds that produces relatively intense fluorescence upon irradiation with light generated by lasers used in screening robots and confocal microscopes. The synthesis of the labeled analogues starts from parent amines **1a**[29] and **1b**, both of which are obtained in a four-step sequence from commercially available geraniol and farnesol (Figure 1A). After a variety of conditions were tested, the best yields for the attachment of the fluorescent NBD group were obtained using an inorganic base in an acetonitrile/buffer solvent mixture. Acid-catalyzed removal of the THP-protecting group furnished the desired fluorescent alcohols in good yields. Transformation of these into chlorides **4a**[33] and **4b** was achieved quantitatively using the Corey−Kim reaction. Finally, conversion into the target diphosphates was achieved by nucleophilic substution with tris(tetra-*N*-butylammonium) hydrogenpyrophosphate **5** followed by cation exchange to give the ammonium salt.[32] Purification of the diphosphates **7** by C18 column chromatography afforded the target compounds in 61−69% yield. The diphosphate structure was verified by $^1$H NMR and $^{31}$P NMR as well as by mass spectrometry. The resulting compounds were designated NBD-GPP (**7a**) and NBD-FPP (**7b**).

**Interaction of NBD-GPP and NBP-FPP with Prenyltransferases.** The fluorescence spectra of NBD-GPP and NBD-FPP had excitation maxima at 487 nm and emission maxima at 550 nm (Figure 2). Addition of excess FTase, GGTase-I, or RabGGTase to a solution of NBD-GPP or NBD-FPP resulted in large fluorescence changes. Surprisingly, the sign of this change varied depending on the transferases. Thus, while addition of GGTase-I resulted in a fluorescence increase of 275%, the addition of FTase or RabGGTase resulted in fluorescence quenching by 75% and 70%, respectively (Figure 2). Addition of an excess of GGPP or FPP to the mixture resulted in reversal of the signal change and return of the fluorescence to the original level, indicating that the fluorescence signal change indeed reflected specific interaction of the developed compounds with the active sites of the enzymes (data not shown). The large changes in fluorescence allowed us to determine the affinity of prenyltransferases for the analogues. Titrations of NBD-GPP or NBD-FPP with prenyl transferases are shown in Figure 2. In the case of RabGGTase, 200 nM NBD-Fpp was titrated with increasing concentrations of enzyme. For the other two prenyltransferases, GGTase-I and FTase, titration of the same concentration of NBD-labeled lipid gave steep curves with sharp kinks, indicating much tighter binding (not shown). To determine more accurately the binding constants for these two enzymes, the concentrations of NBD-FPP and NBD-GPP were lowered to 20 and 50 nM, respectively. The experimental data were fitted using a quadratic equation, yielding $K_d$ values of 1.6 ± 0.1 nM for the FTase:NBD-GPP interaction, 6 ± 1 nM for GGTase-I:NBD-FPP, and 328 ± 9 nM for RabGGTase:NBD-FPP (Figure 2).

While the determined affinities of FTase and GGTase-I for fluorescent isoprenoids are close to those for the native substrates, RabGGTase bound NBD-FPP ca. 30-fold more weakly than it bound GGPP.[38,41,42]

Among many other utilities, the fluorescent analogues offer a convenient method for the determination of the enzymes' affinity for their native substrate.[39] We decided to test this approach on GGTase-I, whose affinity for GGPP was determined previously only by a gel filtration assay.[43] 200 nM of NBD-FPP was mixed with 200 nM GGpp, and the resulting solution was titrated with increasing concentrations of GGTase-I. As can be seen in Figure 3, there was an initial lag in the fluorescence increase, explained by GGPP binding more strongly than NBD-FPP to the transferase, initially resulting in the formation of a fluorescently silent complex. The data were fitted numerically with the program Scientist using a previously described approach[39] and led to a $K_d$ value of 0.25 ± 0.01 nM for the GGPP:GGTase-I interaction (Figure 3).

This demonstrates the utility of the developed fluorescent analogues for studies of prenyltransferase:lipid substrate interactions and shows that GGTase-I binds its lipid substrate significantly more tightly than was previously believed (16 nM).[43]

**NBD-GPP and NBP-FPP Function as Efficient Prenyl Donors for Prenyltransferases.** Following the observation that NBD-FPP and NBD-GPP can bind to prenyltransferases in a mode similar to that of native phosphoisoprenoids, we set out to determine whether these compounds could also serve as lipid donors for these enzymes. To this end, we performed an in vitro prenylation reaction in which enzymes were mixed with their corresponding fluorescent isoprenoid substrates and Rab1A, Rab7, RhoA, or Ki-Ras4B GTPases fused to GST. Control samples were supplemented with an excess of GGPP or FPP that would compete with the fluorescent analogues and thus yield nonfluorescent prenylated GTPases (see Materials and Methods for details).

The reaction was allowed to proceed for 15 min at room temperature and was quenched by addition of SDS-PAGE

(41) Furfine, E. S.; Leban, J. J.; Landavazo, A.; Moomaw, J. F.; Casey, P. J. *Biochemistry* **1995**, *34*, 6857−6862.
(42) Yokoyama, K.; Zimmerman, K.; Scholten, J.; Gelb, M. H. *J. Biol. Chem.* **1997**, *272*, 3944−3952.
(43) Yokoyama, K.; McGeady, P.; Gelb, M. H. *Biochemistry* **1995**, *34*, 1344−1354.

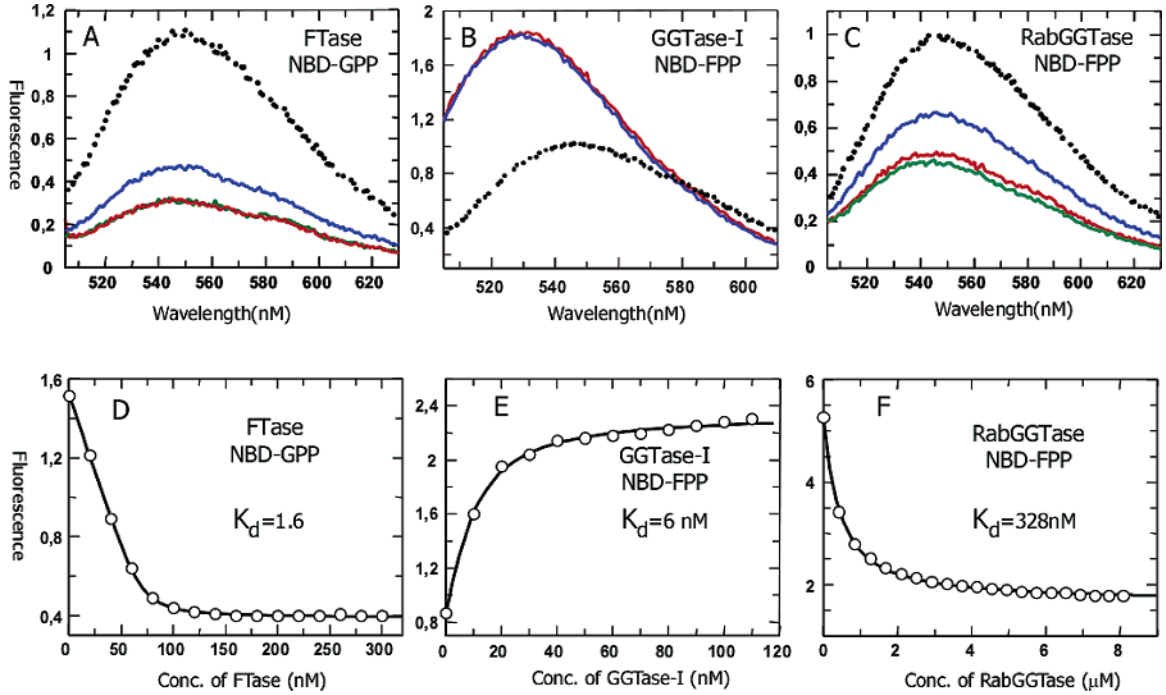


***Figure 2.*** Interaction of NBD-GPP and NBD-FPP with prenyltransferases. (A−C) Emission scans of NBD-GPP (A) and NBD-FPP (B,C) in the absence (small filled circles) and presence of increasing concentrations of prenyltranserases (blue → red → green solid lines). (D) Titration of 50 nM of NBD-GPP with increasing concentrations of FTase. The data were fitted to a quadratic equation as described in Materials and Methods. (E) Titration of 20 nM NBD-FPP with increasing concentrations of GGTase-I. Data were fitted as in (D). (F) Titration of 200 nM NBD-FPP with increasing concentrations of RabGGTase. Data were fitted as in (D).

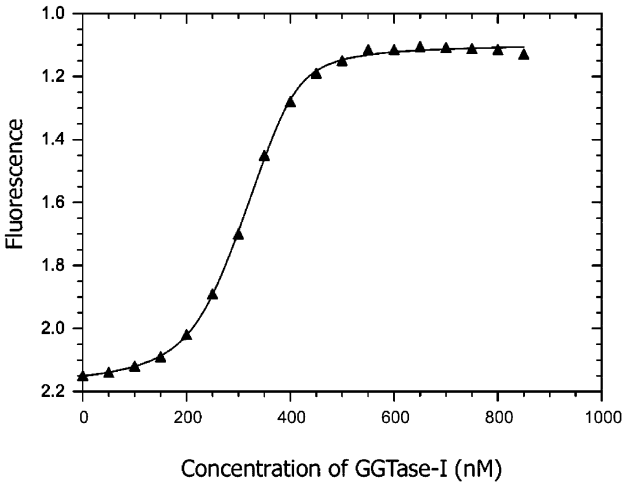


***Figure 3.*** Competitive titration in which 200 nM NBD-FPP was mixed with 200 nM GGPP and then titrated with increasing concentrations of GGTase-I. The data were fitted numerically using the program Scientist. The $K_d$ value for GGPP determined from the fit was 0.25 ± 0.01 nM.

sample buffer, after which the samples were resolved on a 15% SDS-PAGE gel and scanned for fluorescence using a fluorescent image reader followed by Coomassie blue staining. As can be seen in Figure 4, under these conditions incubation of all three prenyltransferases with their respective protein substrates led to emergence of fluorescent bands corresponding to prenylated GTPases. No fluorescent products were generated when either the enzyme or the fluorescent isoprenoid were omitted (not shown). As expected, the reaction was strongly inhibited by excess GGPP or FPP (Figure 4) or by a specific inhibitor (not shown). Therefore, we conclude that the observed fluorescent GTPases do indeed represent specific products of the prenylation reaction. To assess the sensitivity of the method, we loaded decreasing amounts of the prenylation mixture on the SDS-PAGE gel and analyzed it by fluorescent scanning. We were able to detect as little as 6 fmol of fluorescent protein, indicating that the developed methods could be significantly scaled down (data not shown). Fluorescent scanning and quantification of the SDS-PAGE gels loaded with increasing amounts of fluorescently labeled Rab7 showed that the signals remained in the linear range over a 10-fold range of concentrations (not shown).

The sensitivity of the developed assay allowed us to analyze the steady-state kinetics for all three prenyltransferases. Reaction mixtures containing fixed amounts of prenyltransferases and varying amounts of either protein or lipid substrates were incubated for different lengths of time and then resolved by SDS-PAGE. The fluorescence intensity of the bands was analyzed using fluorescent scanning, and the initial velocities of the reactions were fitted with a linear equation (see inset in Figure S1). The obtained rates were plotted against the concentration of the substrates and fitted to the Michaelis−Menten equation (Figures S1, S2). The results are summarized in Table 1. The obtained $K_m$ values reflect the differences in measured affinities of protein prenyltransferase for their respective fluorescent substrates with RabGGTase displaying the highest $K_m$ value of 4.7 $\mu$M and GGTase-I the lowest of 26 nM. Remarkably, the $K_{cat}$ values of all prenyltransferase are in a range of ca. 0.1 $s^{-1}$, which is very close to the values previously measured for protein prenyltransferases.[44−46] This indicates that the basic catalytic mechanism of prenyltransferases

(44) Pompliano, D. L.; Rands, E.; Schaber, M. D.; Mosser, S. D.; Anthony; N. J.; Gibbs, J. B. *Biochemistry* **1992**, *31*, 3800−3807.
(45) Anant, J. S.; Desnoyers, L.; Machius, M.; Demeler, B.; Hansen, J. C.; Westover, K. D.; Deisenhofer, J.; Seabra, M. C. *Biochemistry* **1998**, *37*, 12559−12568.
(46) Zhang, F. L.; Moomaw, J. F.; Casey, P. J. *J. Biol. Chem.* **1994**, *269*, 23465−23470.

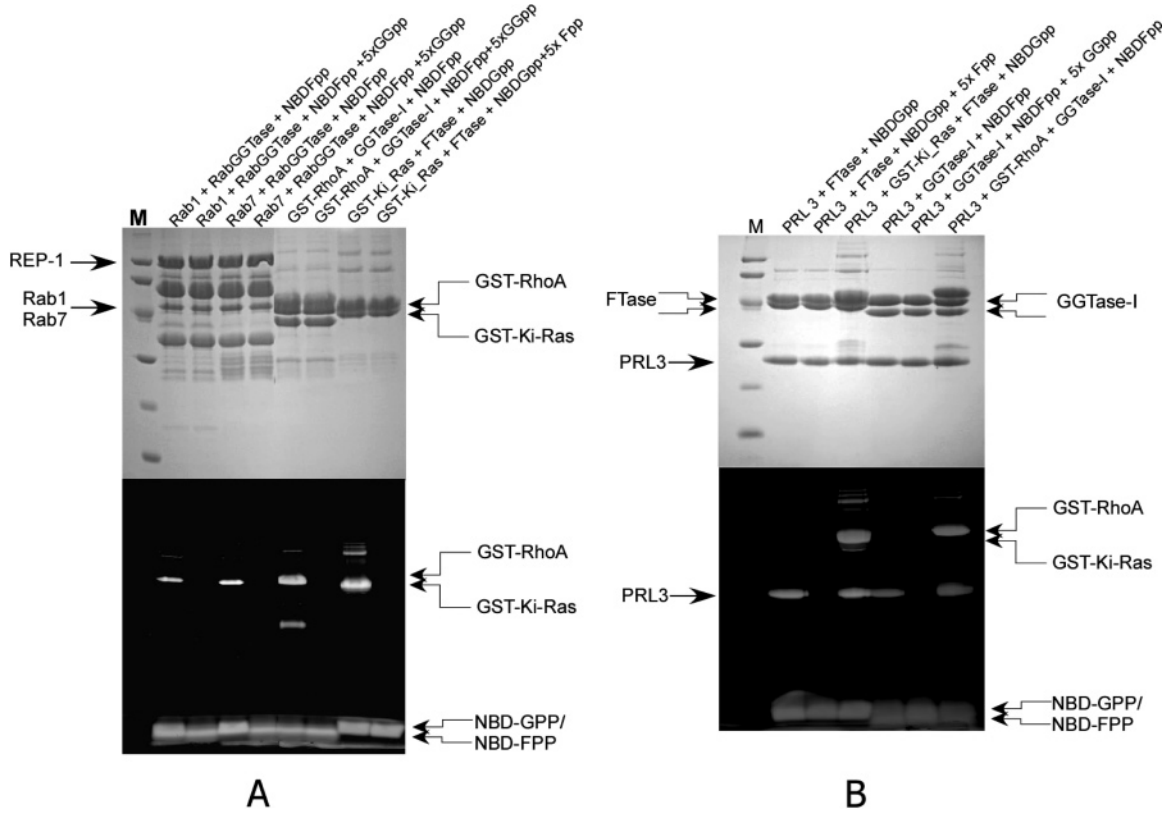


***Figure 4.*** SDS-PAGE gels of the fluorescently labeled GST-Rab1, GST-Rab7, GST-RhoA, GST-Ki-Ras (A), and PRL-3 (B) proteins after prenylation with NBD-GPP and NBD-FPP mediated by prenyltransferases. The control reactions were supplemented with a 5-fold excess of either GGPP or FPP over the fluorescent isoprenoid. Lower panels represent the fluorescent scans of the gels, while the upper panels show the same gels stained with Coomassie blue.

***Table 1.*** Steady-State Kinetic Parameters of the Protein Prenyltransferases with NBD Isoprenoids as Lipid Substrates

| prenyltransferase | substrate | $K_m$ ($\mu$M) | $k_{cat}$ ($s^{-1}$) | $k_{cat}/K_m$ ($M^{-1}\,s^{-1}$) |
|---|---|---|---|---|
| FTase | NBD-GPP | 0.5 | 0.09 | $2 \times 10^5$ |
| | GST-KiRas | 2 | | $0.5 \times 10^5$ |
| GGTase-I | NBD-FPP | 0.03 | 0.08 | $30 \times 10^5$ |
| | GST-RhoA | 42 | | $0.03 \times 10^5$ |
| RabGGTase | NBD-FPP | 4.7 | 0.04 | $0.1 \times 10^5$ |
| | Rab7:REP-1 | 1 | | $0.4 \times 10^5$ |

is not significantly influenced by the substitution of the distal part of the isoprenoid chain with an NBD group (Table 1).

To ascertain that the observations for FTase and GGTase I had general applicability and are not restricted to small GTP binding proteins, we tested a different type of substrate. We chose protein tyrosine phosphatase PRL-3, which is known to be a substrate of FTase in vitro and displays a prenylation-dependent subcellular distribution in vivo. Although this was attributed to the activity of FTase, the potential involvement of GGTase-I cannot be automatically ruled out, given the in vitro evidence for the geranylation of the PRL-1 and PRL-2 homologues of PRL-3.[47] The results of prenylation experiments using FTase and GGTase-I prenyltransferases are shown in Figure 4B. It appears from these data that PRL-3 can be prenylated by both FTase and GGTase-I, although the latter reaction seems to be somewhat less efficient (lanes 1 and 4). In the presence of a 5-fold excess of the corresponding native substrates (FPP and GGPP, respectively), formation of fluorescent products is inhibited (lanes 2 and 5). No prenylation was detected in the case of RabGGTase, which is in accord with the notion of strict specificity of this enzyme for Rab GTPases (data not shown). Our results indicate that PRL-3 may possibly be a dual substrate for both FTase and GGTase-I. Further in vivo experiments should be performed to confirm this in vitro result and to reveal its potential physiological significance.

**Development of a Microscopic Prenyltransferase Assay.** The assay described above provides a significant improvement over the existing prenylation assays due to its simplicity and applicability to all protein prenyltransferases. However, its major shortcoming is in its reliance on SDS-PAGE for detection and quantification of the results, which limits its usefulness for testing larger compound libraries. Therefore, we sought to develop an alternative architecture that could be potentially scaled down and automated. After testing several possible approaches, we chose to use the on-bead assay depicted schematically in Figure 5A.

In this assay, the protein substrate is attached to glutathione-Sepharose beads via a GST tag, and the transferase, fluorescent lipid, and inhibitor are mixed with substrate-loaded beads. If the prenylation reaction occurs, the lipid is transferred to the bead and can be visualized by microscopy using a standard fluorescence microscope. We tested this assay by exposing beads loaded with GST-Ki-Ras fusion protein to a mixture of NBD-FPP and FTase. After incubation, the beads were washed to remove free lipids and viewed under a fluorescence microscope. As can be seen in Figure 5B, beads bearing GST-Ki-Ras appeared brightly fluorescent, while the control beads remained dark. Although the size of the individual beads varied, quantitative analysis of the fluorescence of surface segments of the beads

(47) Zeng, Q.; Si, X.; Horstmann, H.; Xu, Y.; Hong, W.; Pallen, C. J. *J. Biol. Chem.* **2000**, *275*, 21444−21452.

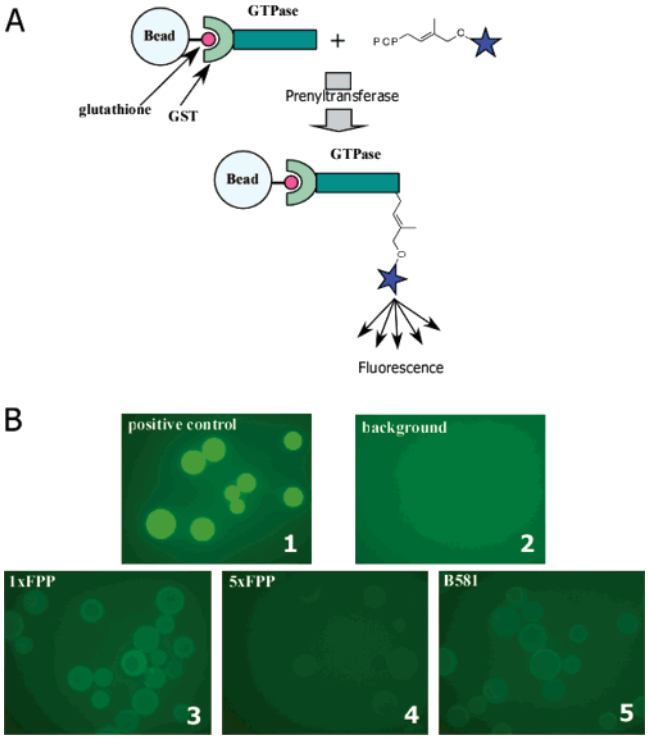


***Figure 5.*** On-bead microscopic assay for identification of prenyltransferse inhibitors. (A) Principle of the assay. (B) On-bead prenylation of GST-Ki-Ras with FTase using NBD-GPP as a substrate. Panel 1, GST-Ki-Ras loaded beads incubated with FTase and NBD-GPP; 2, as in 1 but without FTase; 3, as in 1 but supplemented with an equimolar amount of FPP; 4, as in 3 but with a 5 molar excess of FPP; 5, as in 1 but in the presence of an FTase inhibitor B581.

confirmed that the fluorescence was distributed homogeneously (data not shown). Control experiments using FPP or a competitive inhibitor of FTase (B581) demonstrated that, as in the case of the gel-based assay, the appearance of the fluorescent signal was highly specific (Figure 5B). We repeated similar experiments with RabGGTase and GGTase-I and confirmed that the assay was both sensitive and specific (data not shown).

**Assay Validation and Identification of Novel Prenyltransferase Inhibitors.** To test the applicability of the developed assay in the identification and analysis of novel prenyltransferase inhibitors, we chose a peptidomimetic tripeptide library based on a naturally occurring inhibitor of farnesyltransferase.[34] Among the library members, a number of farnesyltransferase inhibitors with activity in the low micromolar range had been identified by using known fluorescence- and radioactivity-based assays.[34] The simultaneous inhibition of GGTases by these compounds had not been tested so far. For the assay validation test, we selected nine compounds that were highly water-soluble and could be tested in the assay over a broad range of concentrations (data not shown). The selected compounds were added to the prenylation reactions at 20-fold excess over fluorescent isoprenoid, and reactions were developed and measured as described above. As can be see in Figure 6A, several of the tested compounds displayed inhibitory activity toward the prenyltransferases. Interestingly, the presented results demonstrate that the inhibitors showed different potency and specificity toward different prenyltransferases. For instance, inhibitors 670 and 650 appear to inhibit all three prenyltransferases, while compounds 651 and 672 are active only toward FTase and GGTase-I. Analysis of the structures shows that a substitution of tyrosine at position 1 of compound 670 to histidine (see compound 651) or phenylalanine at position 2 to tyrosine (see compound 672) leads to loss of activity toward RabGGTase, while having no significant effect on the activity toward GGTase-I and FTase (Figure 6B).

We chose the compounds with the most pronounced activities for further analysis and determined their $IC_{50}$ values toward the most susceptible enzymes. We performed in vitro prenylation experiments in solution in the presence of increasing concentrations of inhibitors, as shown for 670 and RabGGTase in Figure 7. By plotting the fluorescence intensities of the bands against the concentration of inhibitor, we could determine the $IC_{50}$ values valid for the conditions used (Figure 7 and Table 2). From these data of Table 2, it appears that compounds 650 and 670 are potent inhibitors of GGTase-I/FTase and RabGGTase, with $IC_{50}$ values in the low micromolar range, which would qualify these substances as hits in the search for possible lead compounds. Compounds used in this study were previously tested for inhibition of FTase using a continuous fluorescent assay.[34] With one exception, the results of the bead-based assay correlate well with those of the continuous fluorescent assay. For example, compounds 670 and 650 are shown to display $IC_{50}$ values of $>50$ and 13 $\mu$M toward rat FTase.[34] The only exception is compound 623 that was inactive in the bead assay but was shown to display $IC_{50}$ of 9 $\mu$M for rat FTase. The reason for this is currently unclear and requires further investigation. The results imply that the developed bead-based fluorescent assay provides sensitivity and selectivity comparable to that of other established prenyltransferase assays. Although the assay was employed here essentially in a qualitative manner, calibration of fluorescent intensities of the beads would enable more quantitative use.

**Interaction of Compounds 650 and 670 with FTase.** The obtained $IC_{50}$ values provide an indication of the inhibitory activity of the identified compounds under the chosen conditions but do not provide direct information on either their mode of action or their affinity for prenyltransferases. To obtain initial insights into the mechanisms of action of compounds 650 and 670, we chose to test them against the two most distantly related prenyltransferases, FTase and RabGGTase. To determine whether the identified inhibitors compete with the FTase peptide or lipid substrates, we took advantage of the well-characterized fluorogenic FTase substrate dansyl-GCVLS.[48]

Addition of FTase to the peptide solution excited at 329 nm resulted in a large (ca. 3-fold) fluorescence intensity increase and blue shift that could be used for titration experiments. Using this signal change, we obtained a $K_d$ value for the FTase:dansyl-GCVLS interaction of ca. 8 $\mu$M (Figure 8A), rather higher than the value of 1 $\mu$M reported for the FTase:peptide substrate interaction.[41] To test the effect of compound 650 on this interaction, the inhibitor was titrated to a mixture of FTase (17 $\mu$M) in large excess over the fluorescent peptide (384 nM). As shown in Figure 8B, there was a decrease in fluorescence, consistent with dissociation of the peptide from FTase. However, this displacement is not complete, as can be seen by comparison of the data of Figure 8A, which indicate that the fluorescence should be decreased by more than a factor of 2 under the concentration conditions used if complete dissociation occurred.

(48) Pompliano, D. L.; Gomez, R. P.; Anthony, N. J. *J. Am. Chem. Soc.* **1992**, *114*, 7945−7946.

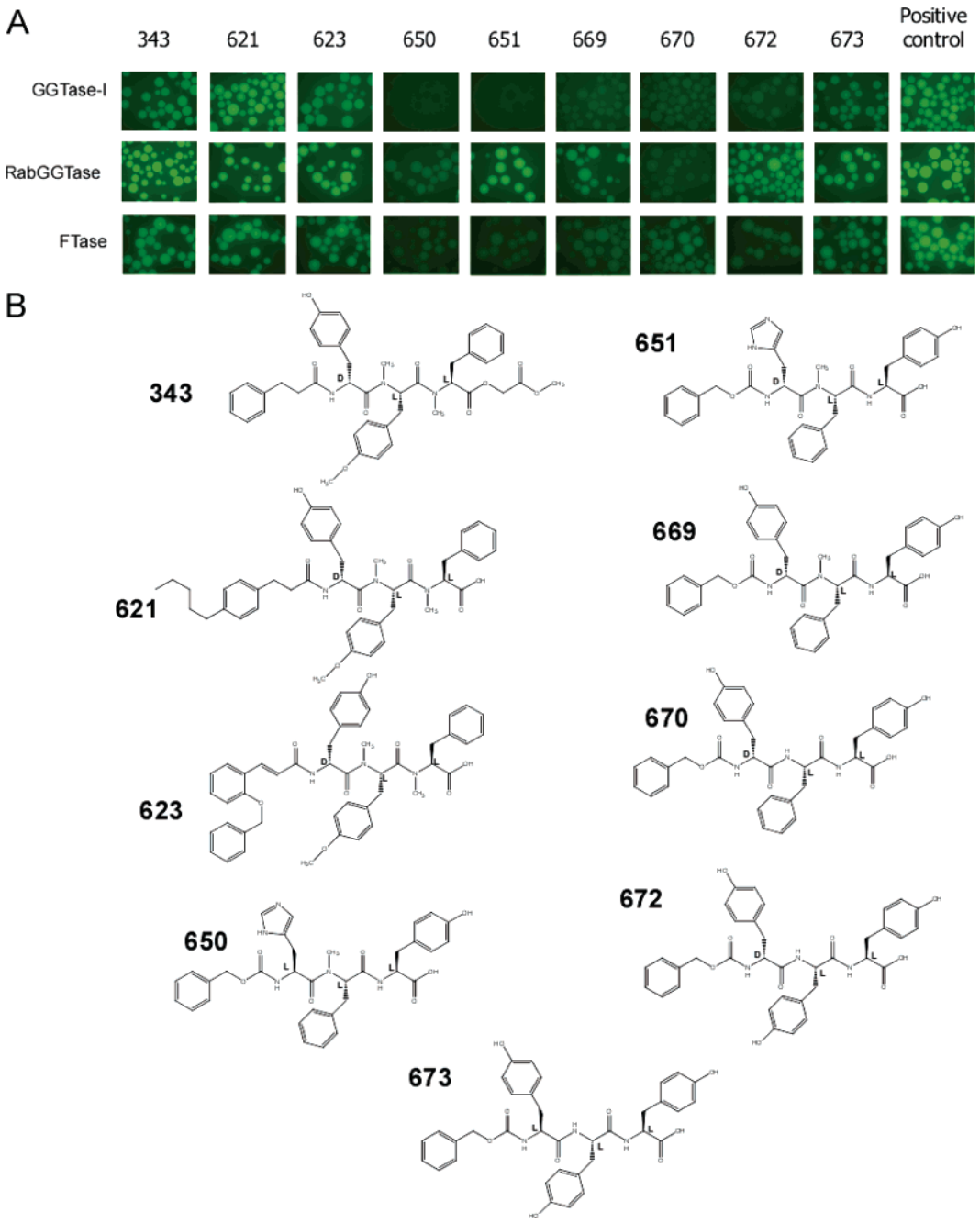


***Figure 6.*** Identification of prenyltransferase inhibitors in the library of tripeptide compounds. (A) Fluorescence of GST-GTPase loaded beads after the prenylation reaction with prenyltransferases and NBD isoprenoid in the presence of putative inhibitors. The samples denoted as positive controls were incubated with buffer only. (B) Structures of the tested compounds.

This result shows that direct competition between peptide and inhibitor binding does not occur, and does not allow distinction between a mechanism in which the two ligands bind simultaneously with mutual weakening of binding, and one in which the fluorescence intensity of the peptide, but not its affinity, is reduced when the inhibitor is also bound. The titration leads to an estimate for the $K_d$ value of compound 650 (ca. 100 nM), because at the very low concentration of peptide used this essentially acts as a tracer and monitors the interaction between FTase and 650. The question of the exact nature of the effect of inhibitor binding on peptide binding is partially answered by the experiment of Figure 8C, in which the titration of FTase against fluorescent peptide was repeated in the presence of a high concentration of compound 650. There is obviously a marked negative effect of the inhibitor on peptide binding, but it was not possible to accurately determine the apparent $K_d$ value under these conditions reliably because saturation was not achievable at the highest concentrations of FTase that could be used. The data quality was good enough to allow a rough estimate of the $K_d$ value under these conditions ($85 \pm 14$ $\mu$M), and because this was under conditions of a high degree of saturation of FTase by the inhibitor, this gives an approximate value for the actual $K_d$ of the peptide when compound 650 is also bound. This suggests that the inhibitor reduces the affinity of peptide binding by a factor of ca. 5.

Similar experiments with compound 670 showed that it bound a factor of ca. 3 less strongly than compound 650, in agreement

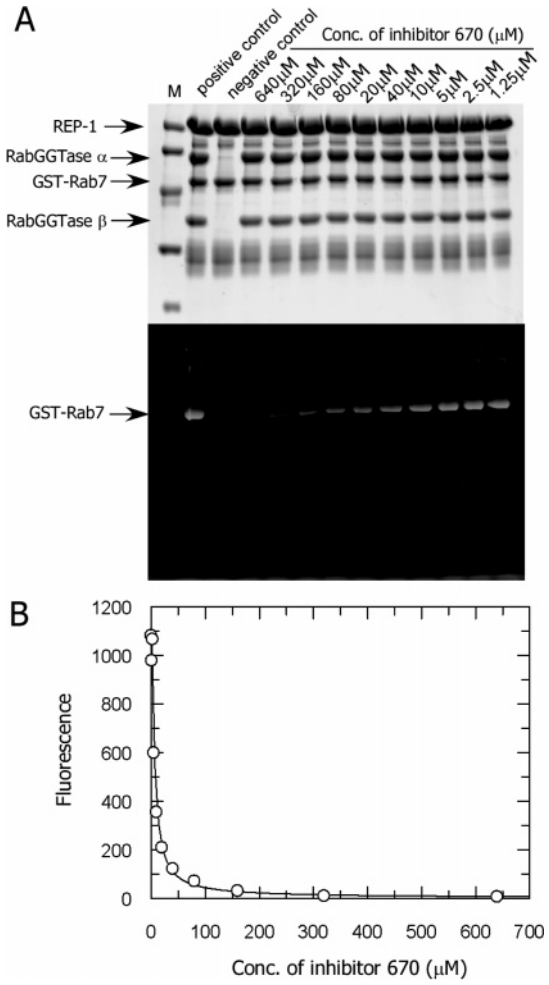


***Figure 7.*** Determination of $IC_{50}$ of the inhibitor 670 for the RabGGTase. (A) The top panel depicts a Coomassie blue stained 15% SDS-PAGE gel loaded with samples for the prenylation reactions containing various concentrations of inhibitor 670. In the negative control, RabGGTase was omitted. The bottom panel shows the fluorescent scan of the gel. (B) Quantification of the prenylation reaction shown in (A). The fluorescence of the GST-Rab7 band was measured and corrected as described in "Materials and Methods", and the obtained data are plotted against the concentration of the inhibitor. The data were fitted to give an $IC_{50}$ value of ca. $5 \pm 2$ $\mu$M.

***Table 2.*** $IC_{50}$ Values of the Tested Compounds toward Prenyltransferases

| compound | prenyltransferase | $IC_{50}$ ($\mu$M) |
|---|---|---|
| 650 | GGTase-I | $1.5 \pm 0.7$ |
| 651 | GGTase-I | $1 \pm 0.3$ |
| 651 | FTase | $80 \pm 38$ |
| 670 | RabGGTase | $5 \pm 2$ |

with the previously measured difference in $IC_{50}$ values where 650 was shown to be ca. 4 times more potent than 670.[34]

Because direct interference with peptide binding cannot completely explain the properties of the inhibitors 650 and 670, we tested the possibility that they might interact with the lipid binding site of the FTase. A mixture of 48 nM NBD-GPP with 57 nM of FTase was titrated with either compound 650 or compound 670. This showed a dose-dependent and saturable increase of fluorescence. Interestingly, the increase of fluorescence saturated before it reached the level of unbound NBD-GPP. If at this point an excess of FPP was added to the reaction, the fluorescence increased to the level of free NBD-GPP and consecutive additions of FPP did not influence the level of fluorescence, indicating that the NBD-GPP was fully displaced (Figure 8D,E). Fitting of the data resulted in apparent $K_d$ values of 1.6 and 3 $\mu$M for compounds 650 and 670, respectively. These results suggest that binding of 650 or 670 to FTase occurs at a site that does not overlap significantly that of NBD-GPP and leads either to a change in fluorescence of bound NBD-GPP or to partial displacement of NBD-GPP, or a combination of both. Further information on this is given by the experiment of Figure 8F, where we performed co-titration experiments in which a mixture of 32 nM of NBD-GPP mixed with 8 $\mu$M of compound 670 was titrated with FTase. When the data was fitted with a quadratic equation, an apparent $K_d$ value of 8.2 nM was obtained (compare this with a $K_d$ value of 1.6 nM for FTase:NBD-GPP interaction).

The concentration of 670 used in this experiment is many orders of magnitude higher than its $K_d$ value, but the effect on the apparent affinity for FTase for NBD-GPP is only a factor of 5, again suggesting a mechanism in which both NBD-GPP and the inhibitor can be bound simultaneously, with relatively weak interaction between the binding sites, presumably by an allosteric mechanism. Fitting the data by numerical simulation to a model in which there is partial competition between binding of the fluorescent lipid and compound 670, and using the values for the affinities of lipid and inhibitor in binary complexes to FTase obtained as described, led to a good fit with a $K_d$ value of 9.7 nM for the interaction of the FTase:670 complex with NBD-GPP (Figure 8F). Thus, the interaction is weakened by a factor of ca. 5 by the presence of compound 670 at its binding site. Interaction of compound 650 with FTase:NBD-GPP complex showed similar behavior, indicating that both compounds have a dual mode of action by competing directly with the weakly binding peptide substrate while also reducing the affinity for the lipid substrate.

The results obtained with compounds 650 and 670 suggest that ternary complexes between FTase, NBD-GPP, and an inhibitor can be formed in which affinities for both substrates are reduced, but not dramatically enough to account for the complete inhibition of prenylation observed. This suggests that binding of inhibitor disturbs the organization of catalytically important residues in the active site in addition to weakening substrate binding.

**Interaction of Compounds 650 and 670 with RabGGTase.** To understand the mechanism by which compounds 650 and 670 inhibited RabGGTase, it would be desirable to perform a set of experiments similar to those described above for FTase. However, the analysis of the inhibitor interaction with the peptide binding site is complicated by the fact that the protein substrate of RabGGTase is the Rab:REP complex and formation of the catalytically competent ternary Rab:REP:RabGGTase complex involves multiple interactions distributed over the complex components.

As the nearest approximation, we chose to analyze the interaction of the Rab7:REP:RabGGTase complex with the inhibitory compounds. To have a fluorescent readout of the binding of the compound to the ternary complex, we used Rab7 protein in which the prenylatable cysteine residues are modified with rhodamine. Rhodamine labeled Rab7 (r_Rab7) displays large changes in its fluorescence upon interaction with REP and RabGGTase.[49] The titration data of 60 nM r_Rab7:REP:

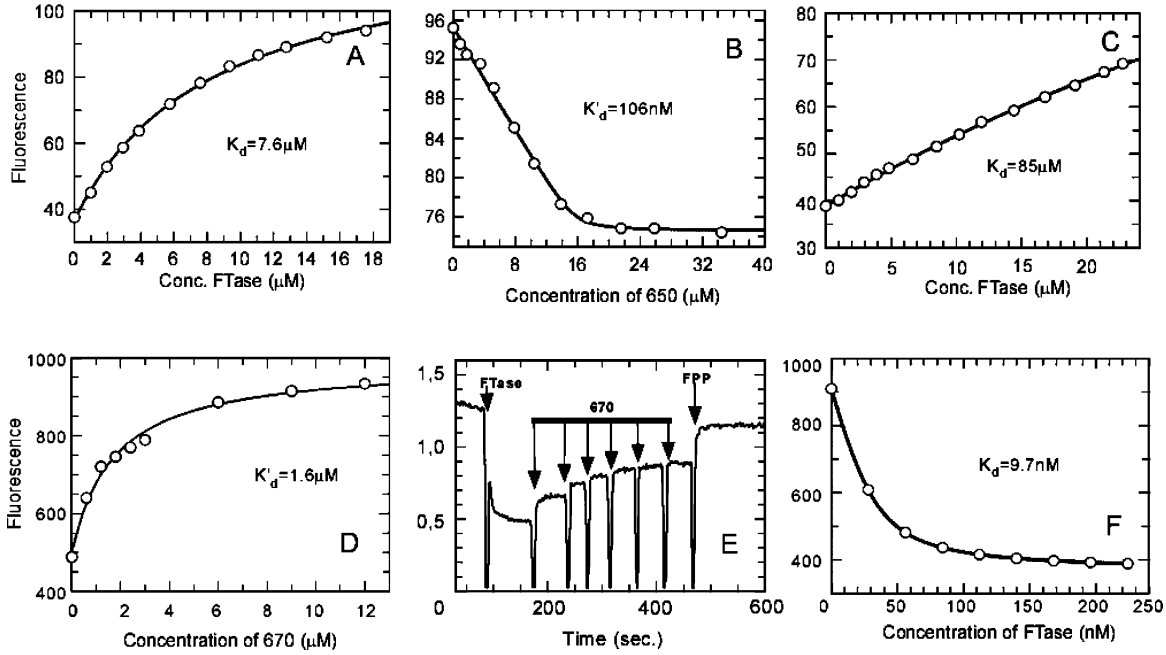


***Figure 8.*** Analysis of interaction of compounds 650 and 670 with FTase. (A) Titration of 385 nM solution of Dans-GCVL with FTase. The fluorescence of the peptide's dansyl group was excited at 329 nm, and the data were collected at 550 nm. The data were fitted with a quadratic equation. (B) Titration of 385 nM Dans-GCVL mixed with 17 $\mu$M FTase with compound 650. The data were processed as in (A) to give an apparent $K_d'$ value of 106 nM. (C) Titration of 385 nM solution of Dans-GCVL with FTase in the presence of 17 $\mu$M of compound 650. The data were processed as in (A). (D) Titration of 48 nM NBD-GPP:FTase complex with compound 670. The data were fitted using the quadratic equation to give an apparent $K_d'$ of 1.6 $\mu$M. (E) Raw data for a titration of NBD-GPP with FTase and then with compound 670. The initial level of the fluorescence signal represents the emission of free NDB-GPP. In the first step, FTase was added to a final concentration of 57 nM. Subsequently, compound 670 was titrated into the cuvette using 0.75 $\mu$M steps. Finally, FPP was added to a final concentration of 10 $\mu$M. (F) Titration of a 32 nM solution of NBD-GPP and 8 $\mu$M compound 670 with FTase. The fit shown is based on numerical simulation with the program Scientist using a partially competitive model (see Supporting Information).

RabGGTase complex with compound 670 are shown in Figure 9A. The observed fluorescence decrease data could be fitted as described above to a $K_d$ value of 650 nM that represents the affinity of compound 670 to the catalytic ternary complex. To assess the compound's potential interaction with the lipid binding site of RabGGTase, we titrated a mixture of 100 nM NBD-FPP and 480 nM RabGGTase with compound 670. As can be seen in Figure 9B, this resulted in a saturable increase of fluorescence. As in the case of the FTase:670 interaction, the fluorescence did not reach the level produced by unbound NBD-FPP and addition of excess of GGPP led to the return of fluorescence to the level of free NBD-FPP (not shown). The fluorescence titration data could be fitted to a $K_d$ value of 1.8 $\mu$M. This value represents the upper limit for the $K_d$ value of the 670 interaction with the RabGGTase:NBD-FPP complex and indicates that 670 is most likely to associate with the peptide binding site of RabGGTase but might have a weak influence, either allosterically or physically, on the lipid binding site. To assess the effect of 670 binding on the affinity of RabGGTase for its lipid substrate, we titrated a mixture of 100 nM of NBD-FPP with 4 $\mu$M 670 with increasing concentrations of the transferase. The data presented in Figure 9C could be fitted to a $K_d$ value of 480 $\pm$ 40 nM, indicating that unlike in the case of the FTase, the interaction of compound 670 with the peptide binding site did not significantly influence the enzyme's affinity for the lipid substrate (compare value of 320 nM for the corresponding $K_d$ in the absence of the inhibitor; Figure 2F), suggesting lack of communication between the binding sites. Thus, the difference between the affinity of 670 for the ternary complex in the absence and presence of NBD-FPP seen in the experiments of Figure 9A and B is probably a result of the different Rab constructs used (wild type and rhodamine labeled, respectively). Interactions of compound 650 with RabGGTase showed behavior similar to that described for 670 albeit with somewhat lower affinity (data not shown).

**Intracellular Delivery and Imaging and in Vivo Conjugation of the NBD-Isoprenoids.** The evident suitability of the NBD-FPP and NBD-GPP isoprenoids for fluorescence imaging prompted us to assess their utility for in vivo experiments. Before attempting the microinjection studies, we tested the ability of both compounds to permeate the plasma membrane of cultured human epidermal carcinoma A431 cells. Already after 5 min of incubation intracellular staining could be observed. To exclude the formal possibility that the observed staining was a consequence of fluid phase uptake, we incubated cells with fluorescent isoprenoids at 0 °C, which ensures complete suppression of intracellular membrane transport. Remarkably, this treatment did not abolish intracellular delivery of the fluorescent compounds, nor did it significantly change their intracellular localization, indicating that isoprenoids were internalized by a process other then fluid phase uptake. The series of confocal optical sections through a group of cells depicted in the movie S1 shows that isoprenoids give diffuse intracellular staining with numerous brightly fluorescent round structures located throughout the cytoplasm (Figure 10A). The isoprenoids were excluded from the nucleus and virtually absent from the plasma membrane. On the basis of these images, we concluded that the isoprenoids were not unspecifically associated with the plasma membrane.

(49) Alexandrov, K.; Simon, I.; Yurchenko, V.; Iakovenko, A.; Rostkova, E.; Scheidig, A. J.; Goody, R. S. *Eur. J. Biochem.* **1999**, *265*, 160−170.

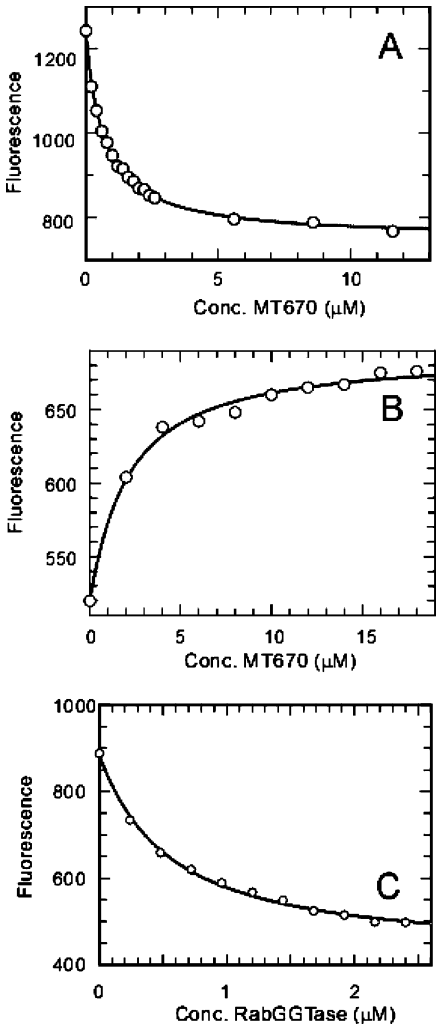


***Figure 9.*** Analysis of interaction of compounds 670 with RabGGTase. (A) Titration of 60 nM rhodamine labeled Rab7 mixed with 90 nM REP-1 and 300 nM RabGGTase with increasing concentrations of compound 670. The data were fitted with a quadratic equation leading to an apparent $K_d$ of 650 nM. (B) Titration of a 100 nM solution of NBD-FPP and 480 nM RabGGTase with compound 670. The data were fitted as in Figure 8D and led to a $K_d$ value of 1.8 $\mu$M. (C) Titration of a mixture of 100 nM solution of NBD-FPP and 4 $\mu$M inhibitor 670 with RabGGTase. The data were fitted as in Figure 8F and led to a $K_d$ value of 480 nM.

Temperature-independent membrane permeability of FPP and GGPP has been previously demonstrated.[50] The details of the process are currently unclear, as it is unknown whether the isoprenoids cross the membrane in the form of pyrophosphates or alcohols. The latter are more likely to be able to cross the membrane because they are much more hydrophobic than the prenyl pyrophosphates. Because the pyrophosphate group of phosphoisoprenoids is very susceptible to pH and phosphatase-mediated hydrolysis, the alcohols can be rapidly generated in the culture medium or on the cellular membrane. However, the fact that absorbed isoprenoids could be incorporated into proteins indicates that even if isoprenoids cross the membrane as alcohols they are rephosphorylated in the cell by an as yet unknown enzyme.[51] Activities that could convert prenyl alcohols into phosphates and pyrophosphates were found in the microsomal fraction of mammalian cells and in plants.[52−54] These observations do not automatically imply that the fluorescent isoprenoids described here would behave in the same way because they may interact differently with membranes or, if dephosphorylated on cell entry, they may not be a substrate of putative isoprenoid kinases.

Because of these uncertainties, we decided to test whether NBD isoprenoids taken up by the cells could serve as prenyltransferase substrates in vivo. The potential pitfalls of such an experiment lie in the low abundance of protein substrates, their long half-life, and the presence of an intracellular pool of native isoprenoids that would efficiently compete for protein incorporation with the fluorescent isoprenoids. To circumvent this problem, we used COS-7 cells transiently transfected with a construct coexpressing an EYFP-Ki-Ras fusion protein, which is expected to be a substrate of FTase in vivo, and a control ECFP-RabGDI fusion protein, which is not expected to be prenylated. Expression of EYFP-Ki-Ras was confirmed by Western blotting with anti-GFP antibody (not shown). To reduce the intracellular pool of phosphoisoprenoids, the cells were pretreated for 24 h with compactin, a potent inhibitor of 3-hydroxy-3-methylglutaryl-CoA reductase.[55]

Transfected cells were incubated with NBD-GPP alone or with mixtures of NBD-GPP and FPP or GGPP for 6 h. After incubation, the cells were lysed, separated on SDS-PAGE gels, and scanned for fluorescence. In the transfected cells pretreated with compactin, a fluorescent band of 48 kDa corresponding to EYFP-Ki-Ras could be observed, while no 80 kDa ECFP-GDI was detectable, showing that fluorescence was a result of an in vivo prenylation reaction. Another ca. 52 kDa band migrating just above it was present in both transfected and untransfected cells and represents the chaperone molecule HSP60 that unspecifically binds NDB isoprenoids on SDS-PAGE (J. Kuhlmann, personal communication). The HSP60 band was detectable regardless of whether cells were treated with NBD-GPP or with NBD-FPP, while the 48 kDa band was observed only in transfected cells treated with NBD-GPP. This strongly suggests that the observed band represents EYFP-Ki-Ras covalently modified with NDP-geranyl by endogenous FTase. To further confirm that the observed 48kDa band indeed represented prenylated EYFP-Ki-Ras protein, we supplemented the cultural medium with an excess of FPP or GGPP. As can be seen in Figure 10B, addition of FPP to the culture medium resulted in an almost complete disappearance of the 48 kDa band but did not affect the signal intensity of the 52 kDa band. In contrast, addition of GGPP to the culture medium did not affect the intensity of the fluorescent EYFP-Ki-Ras band. Remarkably, the fluorescent signal could be efficiently suppressed when the culture medium was supplemented with F-OH (but not GG-OH), indicating that farnesyl alcohol is efficiently transferred across the membrane and converted into pyrophosphate inside the cell (not shown).

The identity of the round intracellular structures accumulating NBD-FPP and NBD-GPP could not be immediately established. Using markers of intracellular compartments, we could exclude

(50) Van Dessel, G.; De Busser, H.; Lagrou, A. *Biochem. Biophys. Res. Commun.* **1997**, *238*, 7−11.
(51) Danesi, R.; McLellan, C. A.; Myers, C. E. *Biochem. Biophys. Res. Commun.* **1995**, *206*, 637−643.
(52) Crick, D. C.; Andres, D. A.; Danesi, R.; Macchia, M.; Waechter, C. J. *J. Neurochem.* **1998**, *70*, 2397−2405.
(53) Bentinger, M.; Grunler, J.; Peterson, E.; Swiezewska, E.; Dallner, G. *Arch. Biochem. Biophys.* **1998**, *353*, 191−198.
(54) Thai, L.; Rush, J. S.; Maul, J. E.; Devarenne, T.; Rodgers, D. L.; Chappell, J.; Waechter, C. J. *Proc. Natl. Acad. Sci. U.S.A.* **1999**, *96*, 13080−13085.
(55) Mendola, C. E.; Backer, J. M. *Cell Growth Differ.* **1990**, *1*, 499−502.

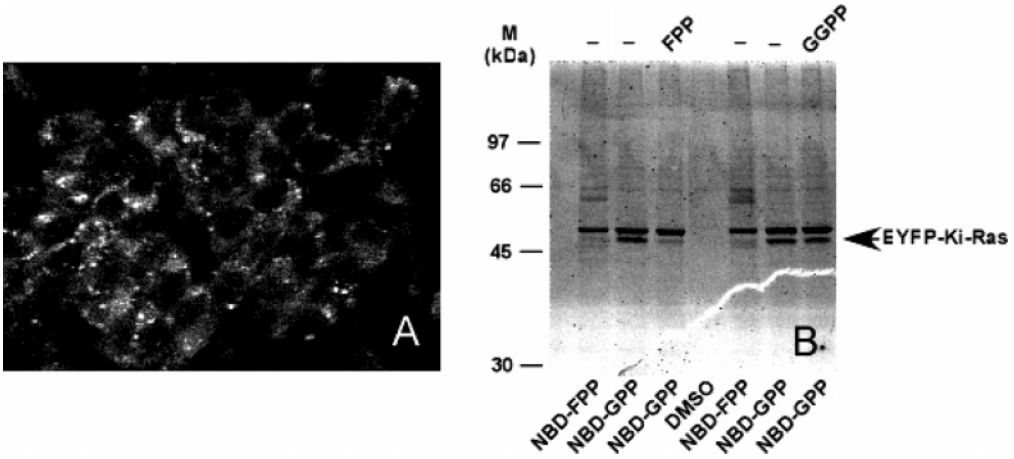


***Figure 10.*** Intracellular delivery of NBD isoprenoids and their incorporation into proteins in vivo. (A) A confocal section image of A431 cells pretreated with 10 $\mu$M NBD-FPP. (B) SDS-PAGE analysis of COS-7 cells transiently expressing EYFP-Ki-Ras and ECFP-RabGDI in the presence of NBD-GPP or NBD-FPP. Cells were pretreated with compactin to deplete the endogenous pool of isoprenods and were then cultured for 6 h in the presence of fluorescent isoprenoids or with DMSO as a control. In competition experiments, culture supernatants were supplemented with GGPP or FPP. Cells were lysed and resolved by 12% SDS-PAGE followed by fluorescent scanning.

that these structures represent the Golgi apparatus and lysosomes (data not shown). It is possible that these structures accumulate the hydrophobic prenyl alcohols that are then converted into the pyrophosphates by resident enzymes. Further work will be needed to clarify the nature and significance of these structures.

## Concluding Remarks

The results presented demonstrate that the developed fluorescent analogues of GGPP and FPP can serve as efficient isoprenoid donors for all three mammalian protein prenyltransferases. They provide new tools for studying interactions of protein prenyltransferases with lipid and peptide substrates and can be used in a generally applicable and potentially numerically scalable in vitro prenylation assay. The presented embodiment of an on-bead in vitro prenylation assay was successfully used to selectively identify protein prenyltransferase inhibitors. The identified inhibitors of protein prenyltransferases showed different affinities and selectivity for individual protein prenyltransferases with some displaying submicromolar affinities for all enzymes. Finally, we show that the synthesized isoprenoids are able to permeate cellular membranes and accumulate in the cytosol and in unidentified vesicular structures of eukaryotic cells. The latter results point to a number of potentially important applications involving mechanisms of membrane permeation, intracellular localization of phosphoisoprenoids, and protein prenylation. This warrants the further development of phosphoisoprenoid analogues, including those furbished with other fluorophores suitable for multicolor in vivo imaging.

**Acknowledgment.** We are grateful to P. J. Casey for a generous gift of cDNAs of FTase and GGTase-I. F. Barr, J. Kuhlmann, R. Ahmadian, and C. J. Vlahos are acknowledged for gifts of cDNAs of Rab1A, RhoA, Ki-Ras, and PRL-3, respectively. Roman Fedorov and Tatjana Dormicheva are acknowledged for the analysis of compound structures and stimulating discussions. This work was supported in part by grant DFG AL 484/5-2 to K.A. and grant I/77 977 of the Volkswagen foundation to K.A., R.S.G., and H.W.

**Supporting Information Available:** Movie S1 of confocal section images of A431 cells pretreated with NBD-FPP. Calibration of the SDS-PAGE-based prenylation assay, steady-state kinetic analysis of protein prenyltransferases, and complete refs 9 and 15. This material is available free of charge via the Internet at http://pubs.acs.org.

JA052196E